Magnetic measurements with the FLASH infrared undulator

O. Grimm[1], N. Morozov[2], A. Chesnov[2], Y. Holler[3], E. Matushevsky[2], D. Petrov[2], J. Rossbach[1], E. Syresin[2]

[1]University of Hamburg, Germany [2]JINR, Dubna, Russia [3]DESY, Hamburg, Germany

19 December 2007

Abstract

The FLASH free-electron laser at DESY, Hamburg, has recently been equipped with an infrared electromagnetic undulator. The device provides radiation in the mid- and far-infrared range. It will be used both for electron beam diagnostics purposes and as a powerful source synchronized to the VUV and soft X-ray pulses of the FEL. This report summarizes the measurements that have been performed prior to installation.

Contents

1 Introduction

The FLASH free-electron laser at DESY, Hamburg, has been equipped during the summer 2007 shutdown with an infrared electromagnetic undulator. The device is tunable over a K-parameter range from 1 to 44, providing radiation up to 200 μm at 500 MeV and up to 50 μm at 1 GeV.

The undulator was manufactured by the Joint Institute for Nuclear Research (JINR) in Dubna, the design being closely adapted to the installation requirements in the FLASH tunnel. Initial functioning tests and characterizations were also undertaken at JINR, followed by more extensive measurements at DESY.

This report summarizes the undulator construction and all measurements that have been performed prior to installation in the FLASH tunnel at JINR and in the magnetic measurement hall at DESY.

2 Undulator construction

The undulator is a planar electromagnetic device with 9 full periods, each 40 cm long. The main parameters are listed in Table 1, a drawing of the undulator integrated into the FLASH tunnel is shown in Figure 1. Figure 2 shows the general design of the undulator. In the following, reference is made to individual poles (the undulator has 44 poles, 22 on upper and lower yoke), to the 22 pole pairs consisting of one upper and one lower pole, and to periods of which the undulator has 9 full ones, each consisting of 2 upper and 2 lower poles. The poles are numbered, starting at the top pole upstream of the electron beam (on the right in Figure 2) and then alternating between up and down.

A high maximum field of 1.1 T is required to reach sufficiently long wavelengths. For the given period length of 40 cm and mechanical constraints, this results in a strongly oversaturated field in the yoke. To stay in the linear regime, a yoke thickness of about 250 mm would be required, but, due to restrictions on weight (imposed by the available lifting equipment) and power consumption, this could not be realized. A yoke thickness of 150 mm was chosen, yielding an oversaturated magnetic field in the steel yoke of 1.9-2.1 T.

2.1 Mechanical design

The magnetic layout of the undulator (Figure 2) consists of 9 regular periods of 400 mm length and special end poles.

The undulator magnetic yoke is made from two ferromagnetic girders of type 1010 plain carbon steel. The poles are milled to 50 μm precision, each is 100 mm wide. The yokes are supported by a C-shaped frame made from non-magnetic steel, limiting a change of undulator gap due to magnetic forces to less than 20 μm. Alignment marks are mounted on the top yoke. The C-shape ensures a free access to the undulator gap from one side.

The excitation coils are wound around the poles. The coils of top and bottom girders are coupled sequentially and powered by a single supply. The first and second poles at both ends have a different number of conductor turns than the main poles.

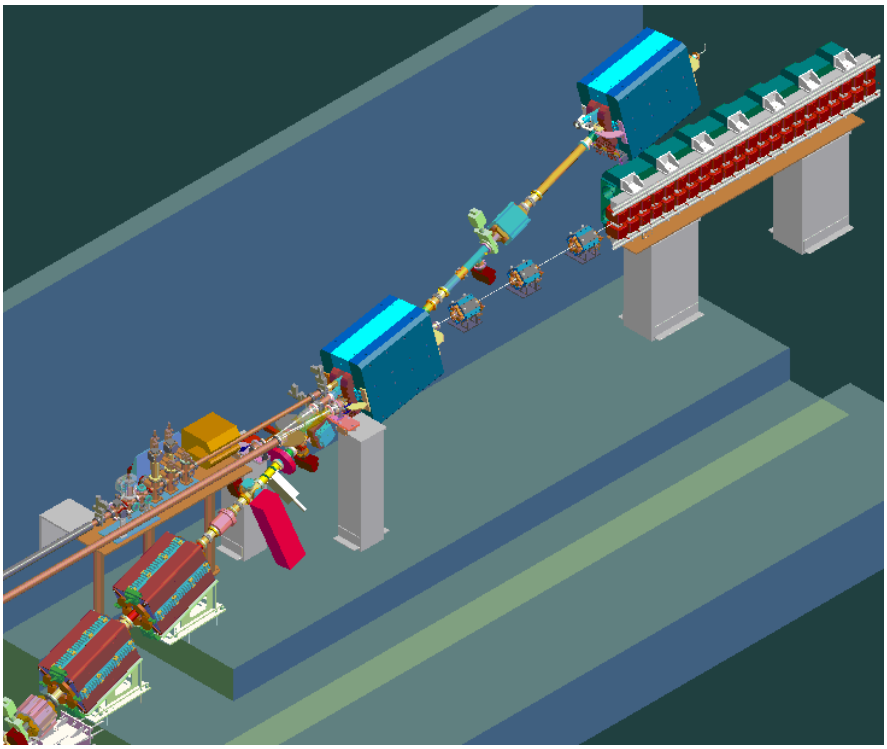

Figure 1 3d view of the infrared undulator in the FLASH tunnel

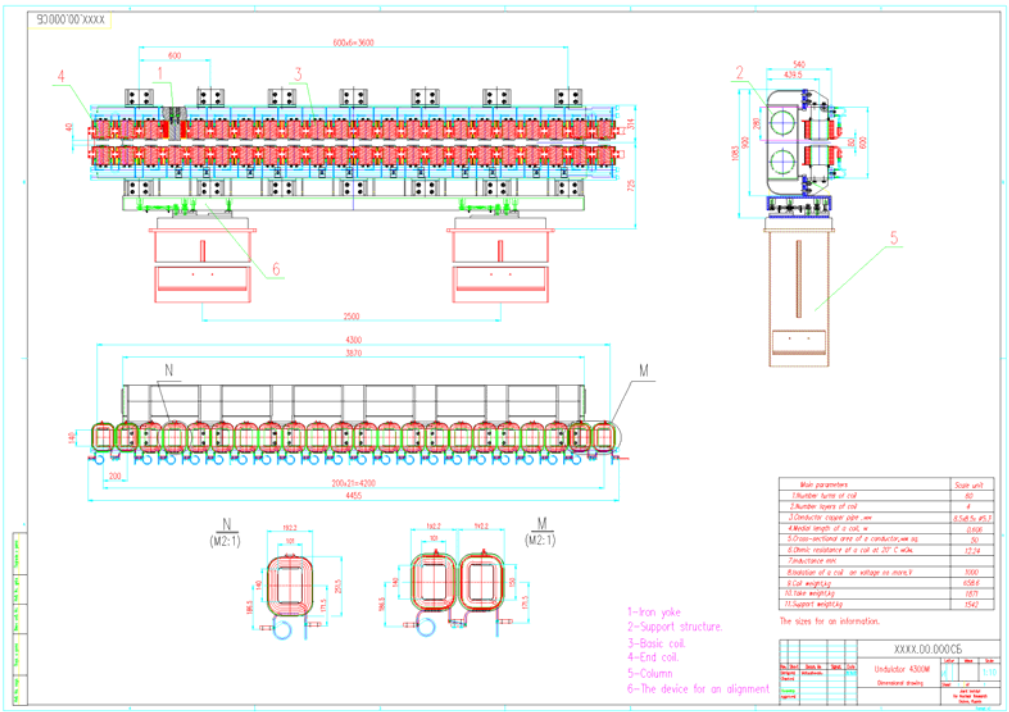

Figure 2 General design of the infrared undulator

Table 1 Design parameters of the infrared undulator

Parameter	Value
Type	Electromagnetic
Gap	40 mm
Period length	40 cm
Pole length/width	10/14 cm
Number of full periods	9
Number of poles	44
End termination pattern	+1/8,-1/2,+1,…,- 1,+1/2,-1/8
Iron yoke length	4.3 m
Overall length including coils	4.455 m
Maximum field	1.2 T
First integral	$<2\cdot10^{-4}$ Tm
Second integral	$<2\cdot10^{-4}$ Tm^2
Maximum K-value	49
Good field region	±10 mm
Total weight	4490 kg
Weight of yoke (steel 1010)	870 kg
coils (copper)	660 kg
support	960 kg
— Main undulator coil —	
Ampere-turns per coil	27840 A
Number of turns	64
Maximum current	435 A
Conductor cross-section	8.5x8.5 mm^2 x Ø5.3 mm bore
Conductor area	50 mm^2
Maximum current density	8.7 A/mm^2
Number of basic/end coils	36 / 8
Resistance (basic coil)	12.36 mΩ
Voltage @ 435 A (basic coil)	5.2 V
Total resistance	0.49 Ω
Total voltage @ 435 A	208 V
Inductance (basic coil)	0.1 mH
Total inductance	4.0 mH
Maximum magnetic force	23700 kg
Water pressure (one coil)	3 bar
Cooling water flow (one coil)	2.25 l/min
Total cooling water flow	100 l/min
Water temperature rise @ 435 A	20°C
Maximum temperature rise (water cut off)	0.4°C/s
Maximum total power	87 kW

— Edge undulator coils —	
Number of turns in first and second coil	10/34
Maximum current	435 A
— Regular corrector coil —	
Number of correction regular coils	36
Resistance	4.1 Ω
Maximum current	2 A
Ampere-turns per coil	540 A
Number of turns	270
Correction of magnetic field at 1.2 T	12 mT

— Edge corrector coils —	
Number of turns in first and second coils	212
Maximum current	15 A
Resistance	0.34 Ω
Correction of magnetic field	60 mT

2.2 Undulator coils

Central main coils

The pole pairs 5 till 18 have coils consisting of four layers of 16 turns each. The windings are made of square copper pipe with 8.5×8.5 mm^2 cross-section and a cooling channel of 5.3 mm diameter (conductor cross-section 50 mm^2). At the maximum coil current of 435 A, the current density is 8.7 A/mm^2. The power dissipated by one regular undulator period (four coils) is 2.54 kW at this current. The insulation thickness between windings is 0.8-1.0 mm (0.4-0.5 mm on each winding). Figure 3 shows the cross-section of such a coil. Each of these coils has additionally 270 turns of correction winding (wire diameter 1 mm, resistance 4.1 Ω), providing a regulation of the Ampere-turns of up to 2% of the maximum value. This permits to compensate perturbations of the magnetic field related to imperfections of the magnetic system. The correction windings are isolated by heat-resistant enamel double coating.

End coils

The first and last pair of coils have only 1/8 of the turns of the central main coils (1 conductor layer, 8 turns), the second and second-last 1/2 (three conductor layers, 32 turns), see Figure 4 and Figure 5. This allows a basic field integral compensation with a minimal corrector coil current in a wide magnetic field range. The end coils are made from the same conductor material as the main coils and power in series with them. The optimum number of turns does not correspond to the usual ratio of ¼ and ¾, as this would result in a more difficult field integral compensation.

The correction windings for the end coils are made from 212 turns of copper wire of 2.5 mm diameter. The resistance is 0.34 Ω, the maximum allowable current 15 A. The correction winding on the first pole pair can provide a field correction up to 60% of its maximum value without correction, the winding on the second pole pair up to 18%.

The main circuit of all 44 coils is powered by one DESY standard power supply MK 506/4.

Due to the oversaturated magnetic field in the yoke at high excitation, the field in the centre of the undulator gap depends on the individual position of each coil. Therefore, each coil position can be adjusted mechanically in the vertical direction within about 1 mm to compensate positioning errors.

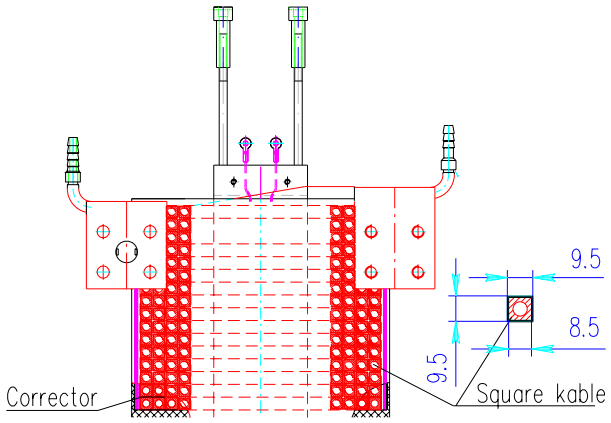

Figure 3 Coil of regular undulator structure with vertical mechanical adjuster

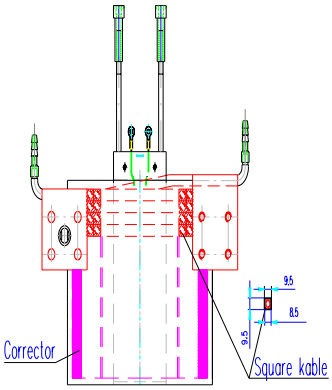

Figure 4 First coil

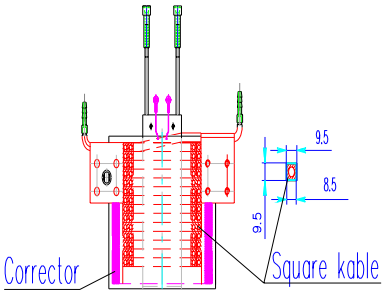

Figure 5 Second coil

2.3 Electrical circuits

The electric schematics of the correction coil circuits is shown in Figure 6. The switches SA1 short-circuit the corresponding coil pair (always one upper and one lower coil), the switches SA2 reverse their magnetic field. The variable resistors Rx are connected parallel to the series of the two coils. These settings are referenced in case they are lost or parts have to be replaced, see Appendix A.

The wiring of the PT-100 temperature sensors[1] and pilotherm switches and their respective connectors is shown in Figure 7. The top and bottom pilotherm switches are connected in one series, each.

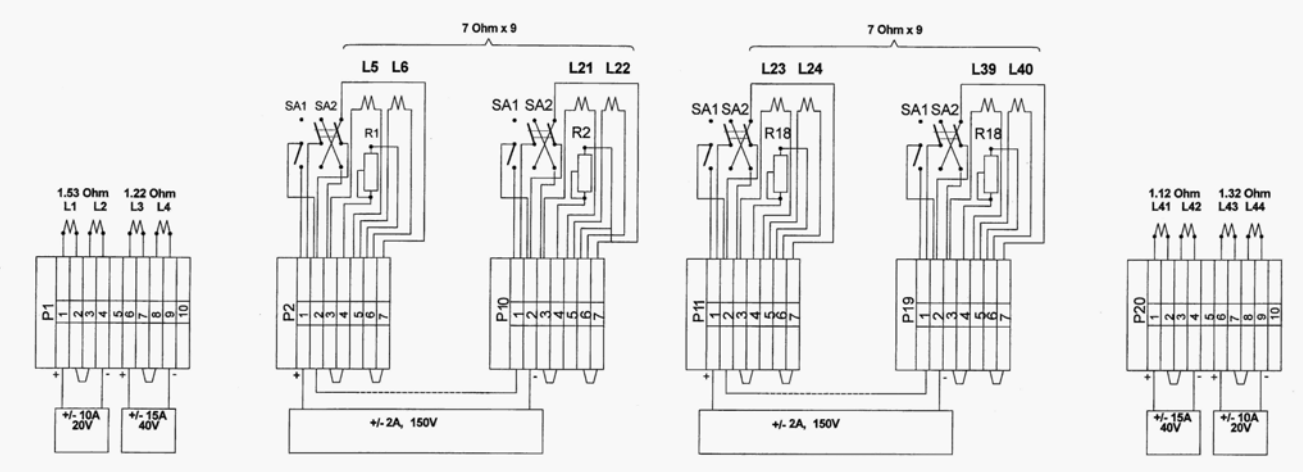

Figure 6 Schematics of correction coils

[1] Microtherm, Pforzheim, Germany, Model EF-1 (two wire) with M4 thread

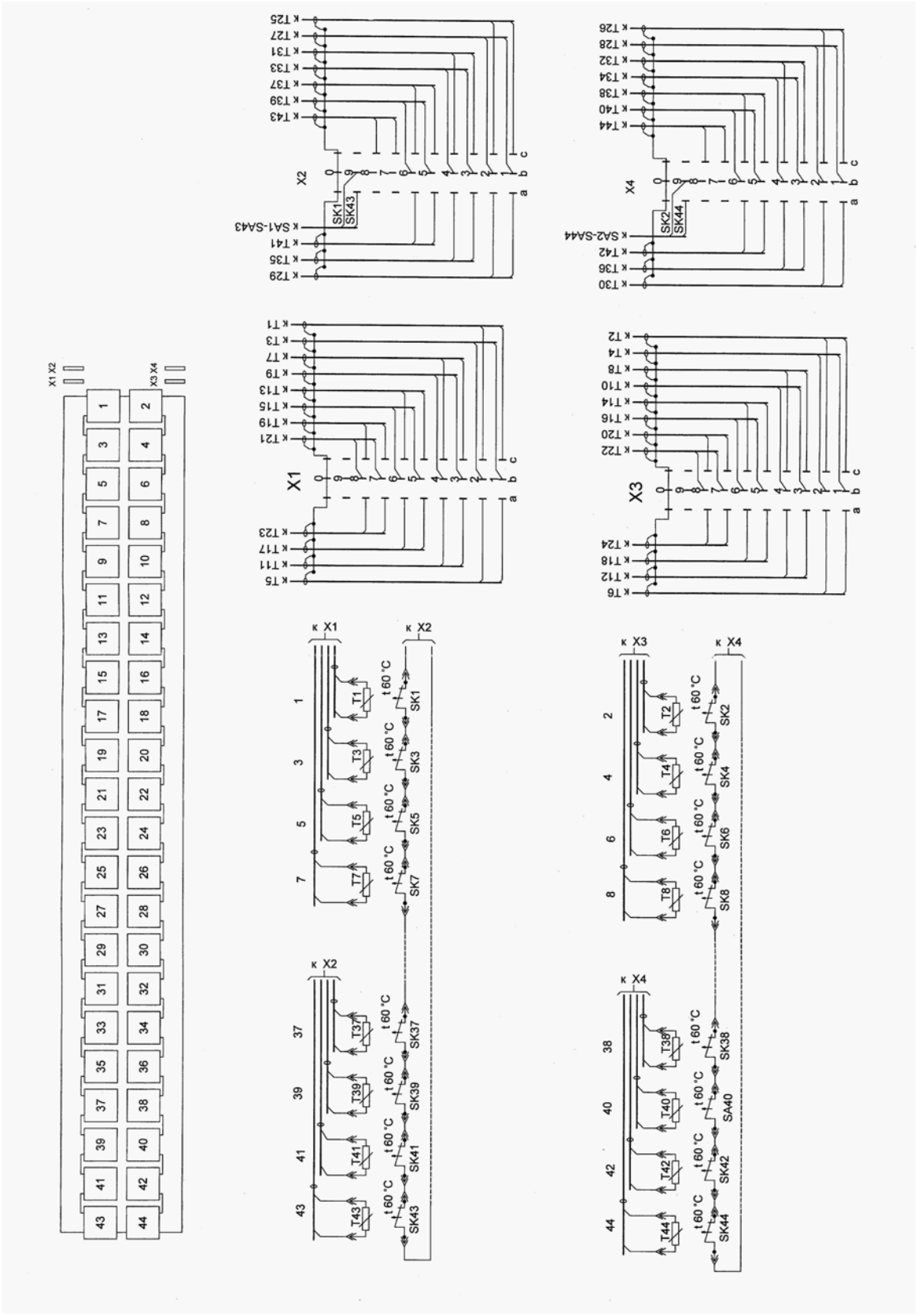

Figure 7 Connection of pilotherm switches and PT-100 temperature sensors

3 Magnetic measurements at JINR

3.1 Measurement bench

The mechanical part of the JINR measurement bench is based on equipment delivered from NIKHEF, Amsterdam. The bench is shown in Figure 8. The 3d measurement head moves in longitudinal direction on rails over a distance of 4.7 m. At the end of the measurement arm the Hall probe is fixed (Figure 9).

Figure 8 View of the measurement bench

Figure 9 Measurement arm with Hall probe

The measurement arm and head are moved with 3 stepping motors (Figure 10). In longitudinal z direction the position of the measurement arm is detected absolutely by a high accuracy (few μm) linear encoder (HEIDENHAIN LIDA-485). For magnetic field mapping a homemade Hall magnetometer HM-16 (Figure 11) was used. The reference magnetic field was measured by a homemade nuclear magnetic resonance magnetometer NM-23 (Figure 12) and a Hall probe MX-12. The probes for both reference magnetometers were installed in the gap of the third pair of undulator poles.

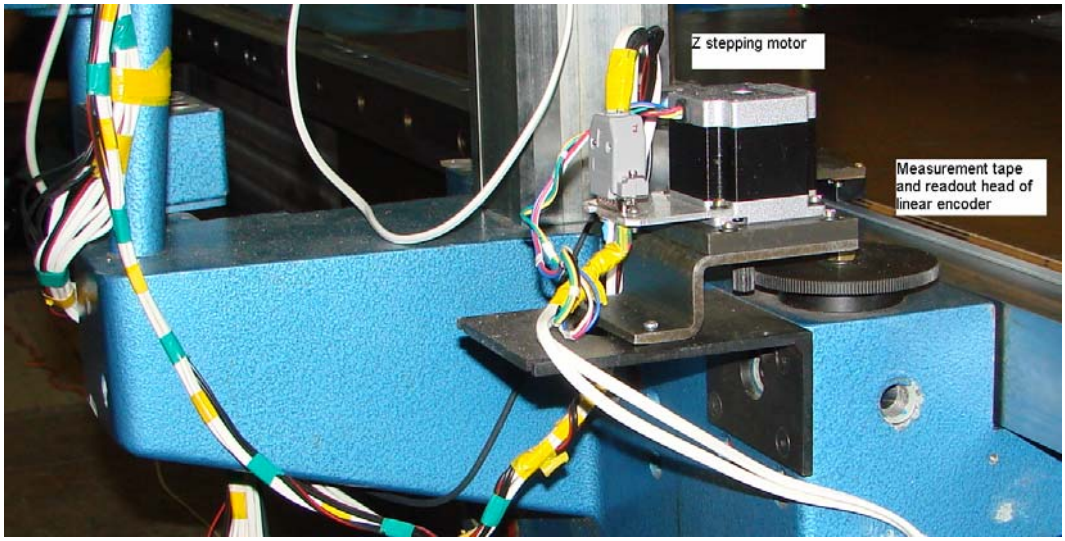

Figure 10 Z stepping motor and linear encoder

Figure 11 HM-16 Hall magnetometer

Figure 12 NM-23 NMR magnetometer

All electronic equipment except the magnetometer MX-12 was controlled by a PC, as shown in Figure 13. The acquired date included time, x, y, z coordinates, and magnetic field measured by the scanning and reference probes. One measurement pass (longitudinal extend 470 cm, step 0.5 cm) required about 2 hours, due to mainly the heavy measurement head and the required delay of 5 seconds for the Hall measurement to settle to a stable value.

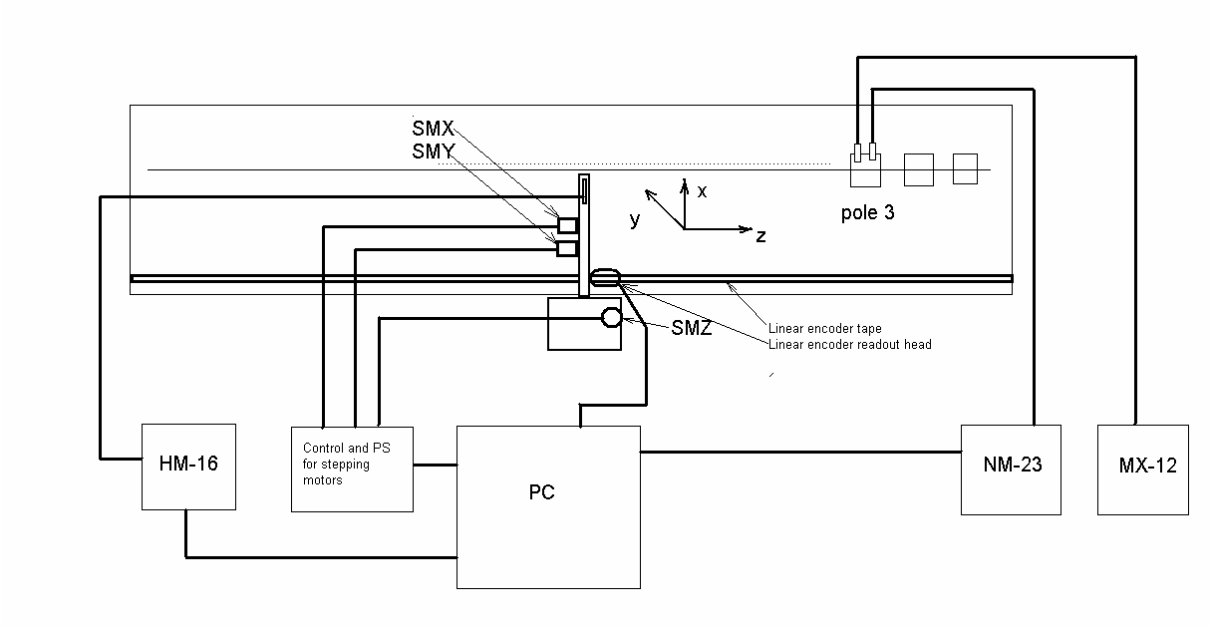

Figure 13 Scheme of the measurement bench hardware

The undulator main coil was excited by a Bruker power supply (450 A,120 V, stability 10^{-5}). Due to the coil resistance, its voltage limit was reached at 200 A excitation current. Correction by the reference probe was not needed for this supply. For excitation currents between 250 A and 380 A, a motor-generator with stability ~10^{-3} was used, requiring correction by the reference probe. Correctors coils were excited with power supplies providing 10^{-3} stability (Figure 14).

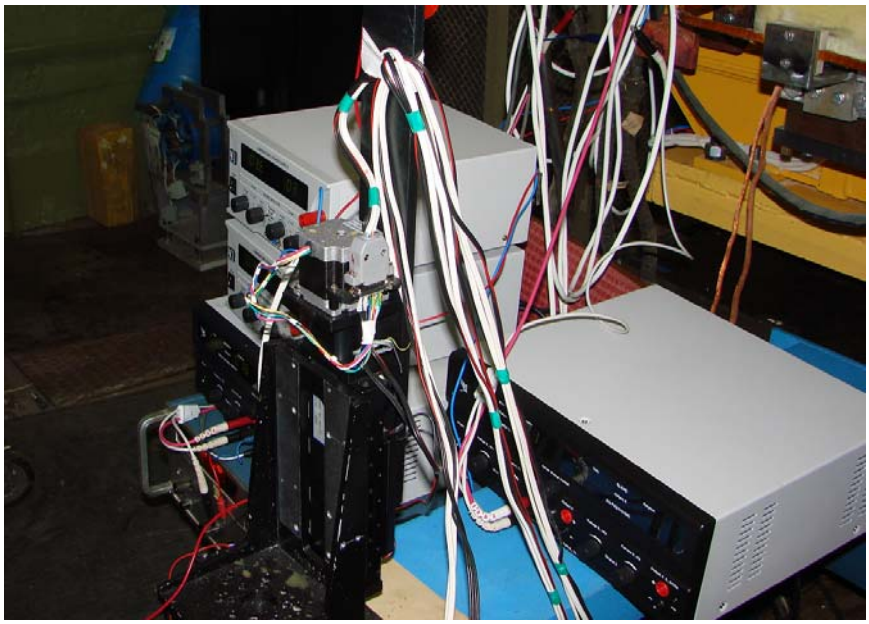

Figure 14 Correction coils power supplies

3.2 Goals of the magnetic field measurements and correction

Initial testing at JINR was geared towards corrections of mechanical, electrical and water cooling problems. Then, a full test of the magnet was done and the system reliability checked. The tuning procedure was along the following guide lines:

- Final first field integral less than 100-200 G·cm, final second field integral less than 200 kG·cm^2.
- First field integral in each regular undulator period less than 100-200 G·cm.
- Second field integral (electron trajectory) along the undulator has an axis as parallel as possible to the undulator axis.
- The above requirements should be fulfilled in the full range of main coil excitation currents between 0 and 435 A.
- Minimization of the number of required correction power supplies.
- The tuning should be reproducible within a deviation of less than 50 G·cm and 5 kG·cm^2, respectively.

3.3 Undulator magnetization curve

The measured magnetization curve (central field, pole pair 4) shows excellent agreement with simulation results obtained with the TOSCA code (Figure 15).

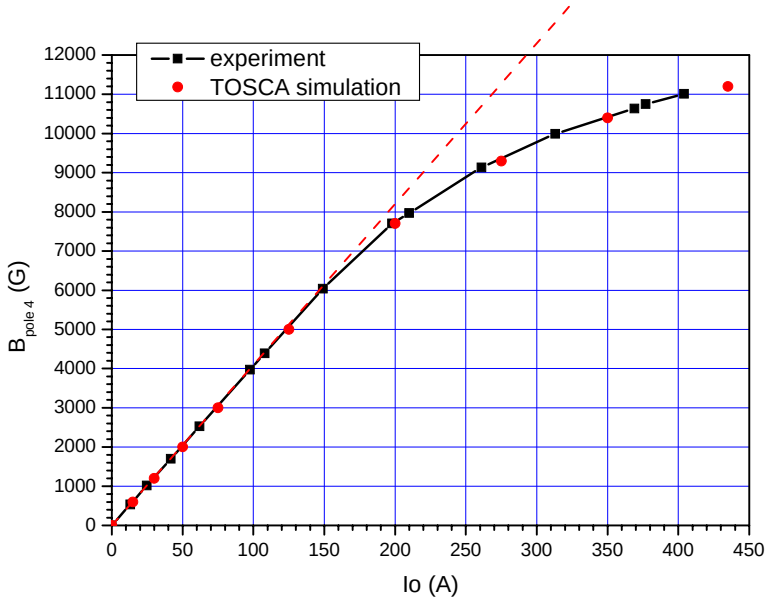

Figure 15 Undulator magnetization curve (pole pair 4)

3.4 Minimization of the first field integral in the regular undulator periods

The first field integral minimization was done in an iterative way by adjusting the values of the correction coil shunt resistors. All regular undulator correctors (poles 3-20) were excited by one power supply in series. The correction was first optimized for a main coil current of 200 A. The resistors were tuned at 1 A correction current. For other main coil currents the value of the regular periods corrector current was then determined which minimized the first field integral. The initial value obtained for the first field integral in the regular periods was 1500 G·cm. The large value results from the difference of the field of individual poles from the average value, see Figure 16. The initial and final values for the first field integral are shown in Figure 17.

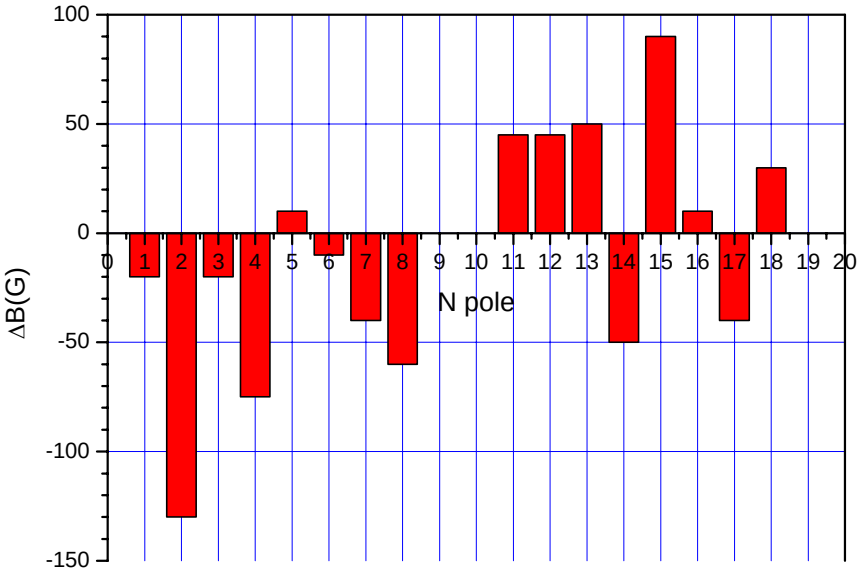

Figure 16 Deviation of the central field for the 18 central pole pairs before tuning

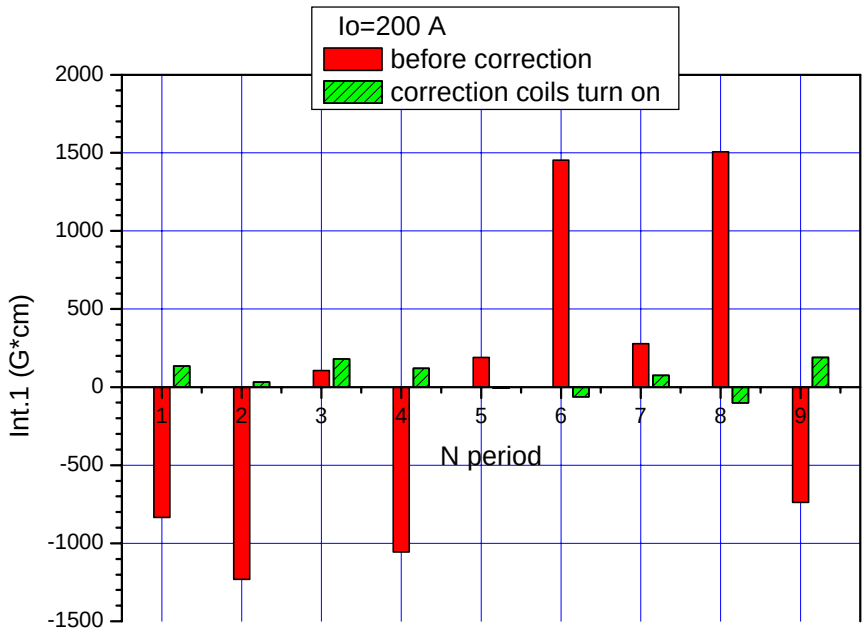

Figure 17 Distribution of the first field integral at 200 A before and after correction coil tuning

The tuning results for the first field integral for all working regimes shaped at JINR are presented in Figure 18. The maximum value of the regular period correction current was below 1.2 A (Figure 19).

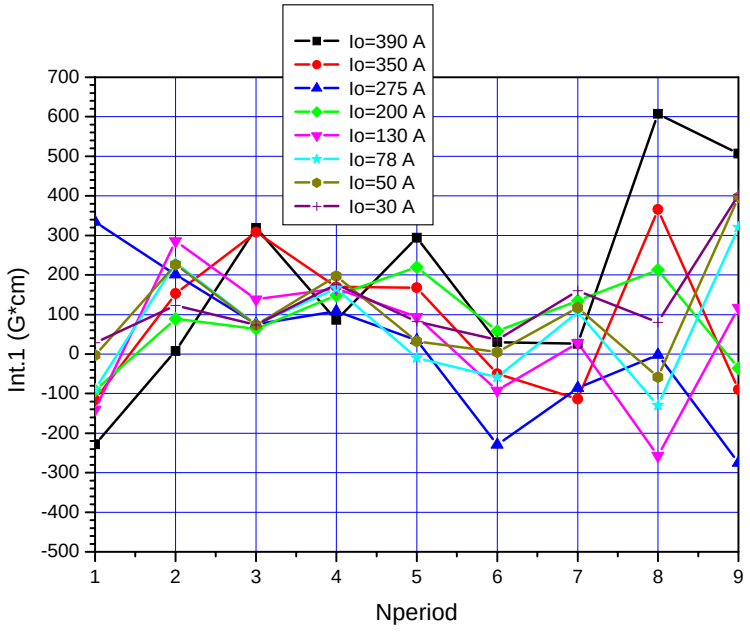

Figure 18 Distribution of the first field integral in the regular undulator periods

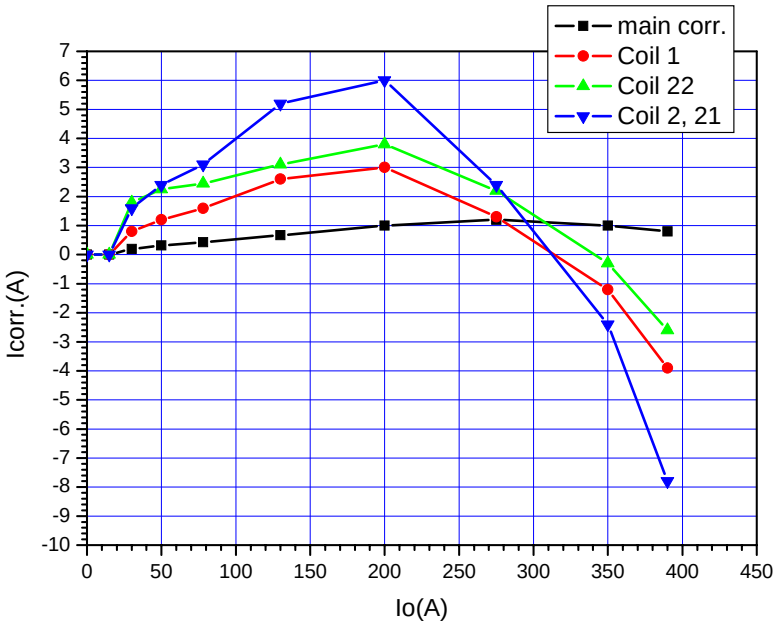

Figure 19 Correction currents for all main coil excitation currents

3.5 Final correction of field integrals and second integral distribution

Final first and second field integral correction and minimization was obtained by tuning the corrector currents for the pole pairs 1, 2, 21 and 22. The maximal correction current was 8 A. The final first and second field integral is shown in Figure 20 and Figure 21.

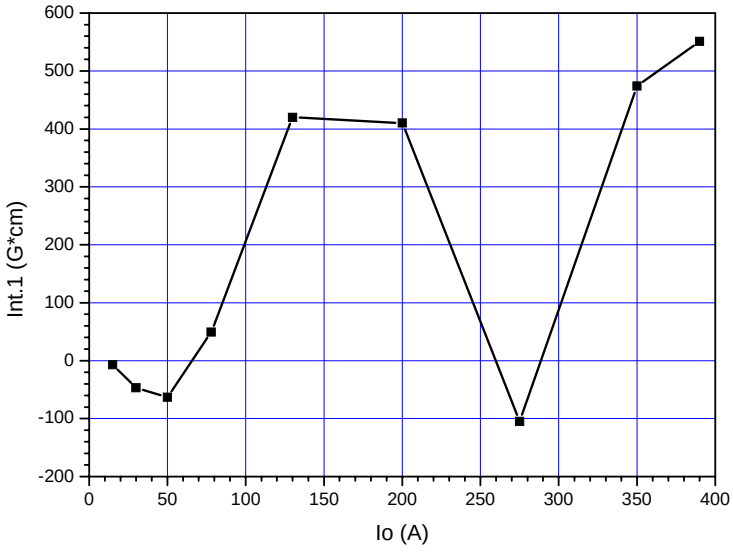

Figure 20 Final first field integral for all main coil excitation currents

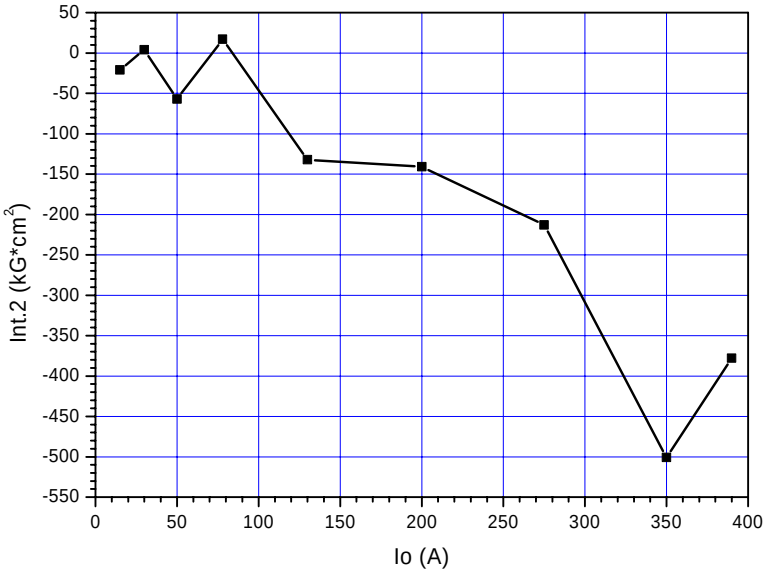

Figure 21 Final second field integral for all main coil excitation currents

The final distributions of the second field integrals are shown in the following figures.

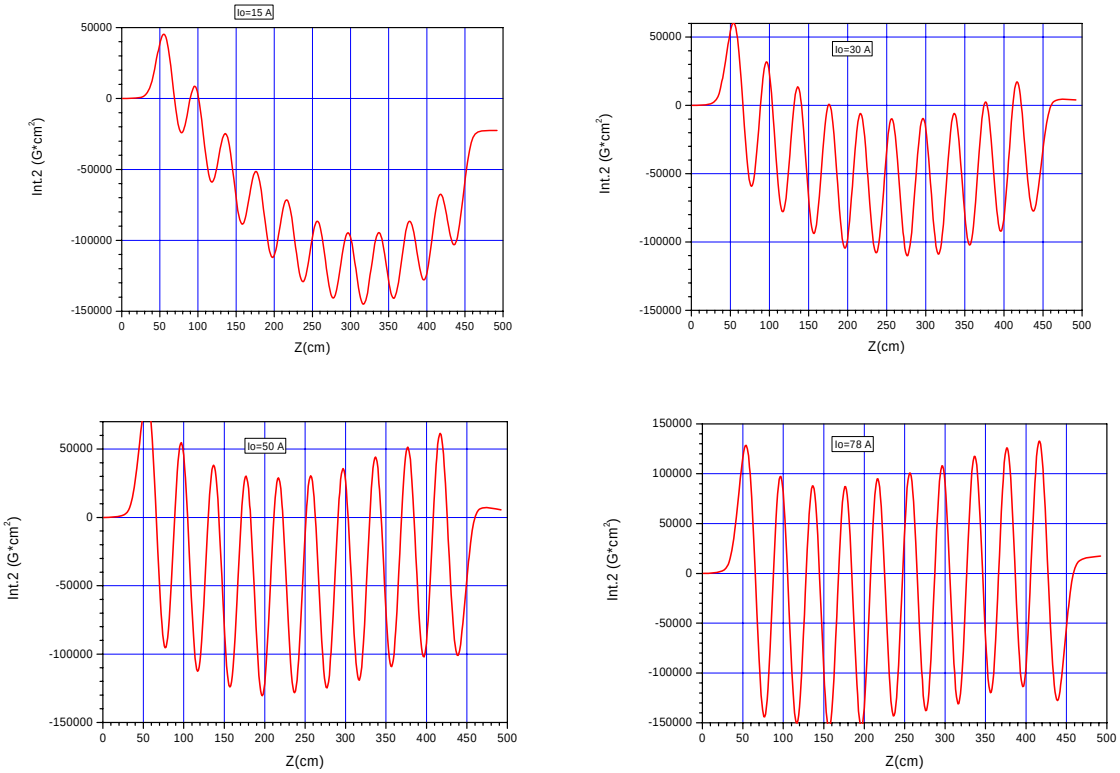

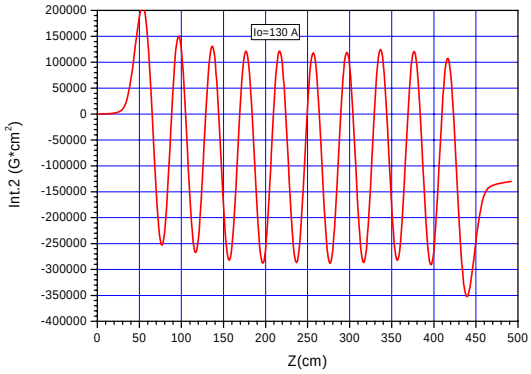
Io=130 A
Int.2 (G*cm^2)
Z(cm)

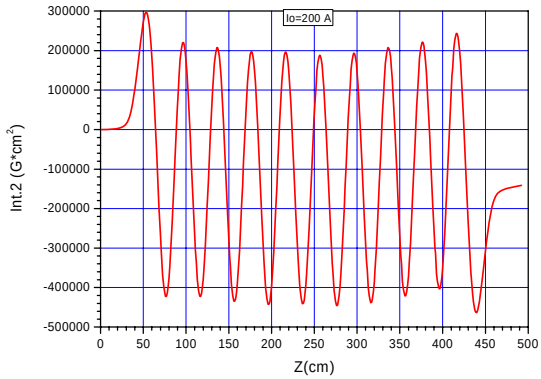
Io=200 A
Int.2 (G*cm^2)
Z(cm)

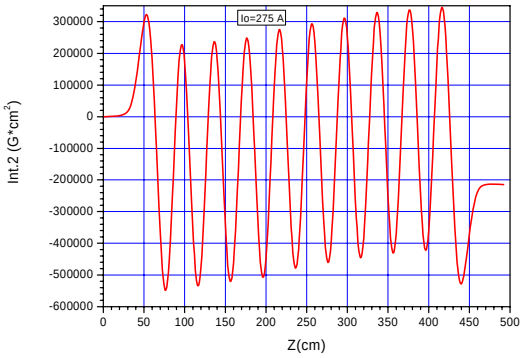
Io=275 A
Int.2 (G*cm^2)
Z(cm)

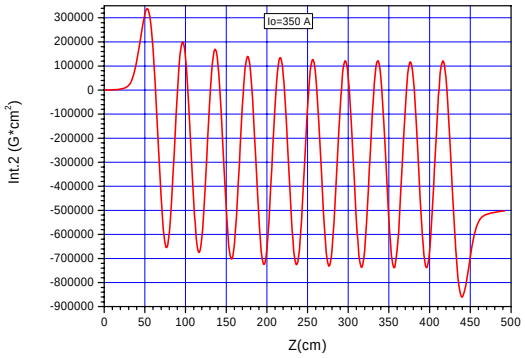
Io=350 A
Int.2 (G*cm^2)
Z(cm)

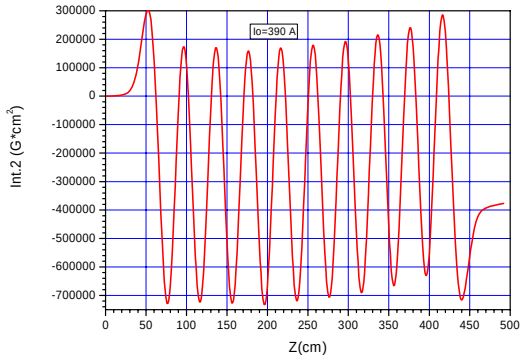
Io=390 A
Int.2 (G*cm^2)
Z(cm)

4 Measurements at DESY

After shipping the undulator to DESY on truck and ferry via St. Petersburg and Kiel, the first measurements intended to verify that the undulator arrived in good shape, without suffering damage or tuning shifts. As a sufficiently stable power supply was available at JINR only for lower main coil excitations currents, the next step was then finishing the tuning for the remaining currents.

As the field mapping at DESY was significantly more rapid than at JINR, the number of main working regimes was increased from 9 to 22. The procedure of working regimes setting was modified (see Chapter 5). Repeatability of the working regimes was studied and 3d maps measured. Repeated measurements of the same regime without changing coil currents have demonstrated an accuracy of determination of the first field integral of ±25 G·cm and of the second of ±5 kG·cm^2. The results of the second field integral shape were very close to the results JINR measurements and a more accurate final value for the first integral was provided at DESY.

4.1 Magnetic measurement bench

The 3d field-mapper is designed to scan the fields of long slim dipole magnets with C-type cross section. The mechanics consist of a 6 m long toothed belt drive linear module for the longitudinal motion (z) with an x-y stage on top for the transverse directions[2]. The units are driven by conventional 2 phase stepping motors with 400 steps/revolution and allow resolutions of 15 μm and 12.5 μm, respectively. The positioning accuracy in z is about (0.1 mm +10^{-4}z) and 10 μm in x and y.

The magnetic field is measured by a precision Hall probe[3] with an accuracy of 1.2×10^{-4}. Its reading is corrected for temperature dependence and nonlinearity. It is mounted to a 400 mm long 8 mm outer diameter carbon fibre tube and can be oriented as to measure one of the 3 field components. A second identical Hall probe in a fixed position serves as a reference sensor to cope with long term drift effects.

The measuring machine is connected to a rack mounted PC equipped with add-on cards for GPIB bus read-out and motion control[4]. The control program is a LabVIEW application. One pass of 5 m through the magnet with 5 mm step width (1001 data points) is completed after about 11 minutes.

The undulator was aligned on the magnetic measurement bench to a precision of 0.5 mm. Pilotherm and water flow interlocks to the main power supply were installed in the same way as for the final tunnel installation.

[2]Franke GmbH, Aalen/Germany
[3]Group3 Technology Ltd., Rosebank, New Zealand, Model DTM-151 with sensor MPT-141
[4]National Instruments, Austin, USA

4.2 Check of reproducibility

A comparison between second field integrals (electron trajectories) obtained before and after shipping is shown for several main excitation currents in Figure 22 and indicates good reproducibility between measurements and JINR and at DESY for the same undulator tuning.

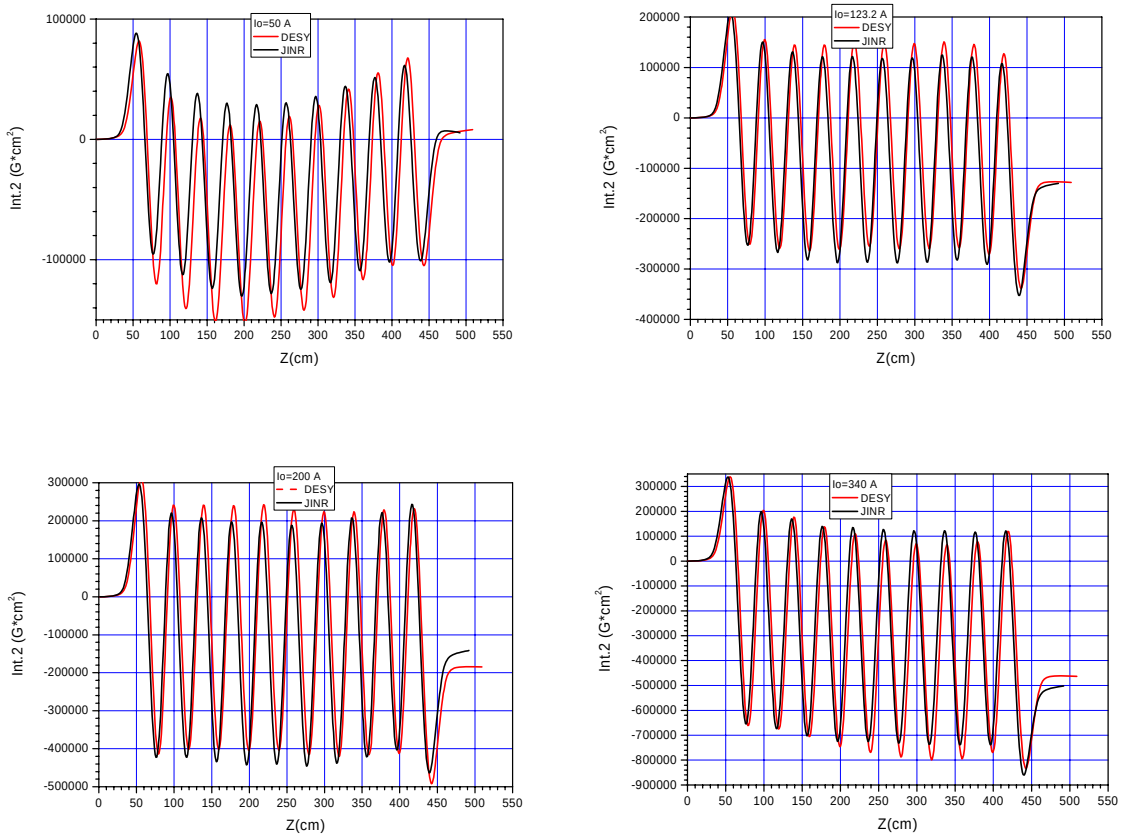

Figure 22 Comparison of second field integrals before and after shipping

4.3 Field measurements at 435 A with thermal isolation

The high power consumption of up to 110 kW and subsequent heating could possibly require dedicated temperature isolation to reduce the amount of heat dissipated into the environment. From the measured water flow rate and temperature rise, less than a few kW are not carried away by cooling water. More precision was not possible as the flow rate could not be measured to better than 5%. Although this is a small number, a thermal shield shown in Figure 23 is available, to be prepared in case higher temperature stability demands in the FLASH tunnel arise in the future.

Within better than 1% no change in output water temperature was measurable with and without thermal isolation at maximum excitation current and constant water flow rate. As the

shield certainly reduces any heat transport to the air significantly, less than 1 kW is actually dissipated into the environment.

The isolation prevents the measurements of field integrals. The Hall probe could only be inserted at several joint points between two layers of the isolation. For one such position centered within one pole pair, the field change over time and with and without thermal isolation has been measured, see Figure 24. The differences are close to the accuracy of the measurement equipment. It also needs to be noted that with isolation present, the Hall probe will be subject to a larger change in air temperature, and thus its temperature coefficient may also start to contribute.

Figure 23 Undulator with thermal shield installed and Hall sensor inserted

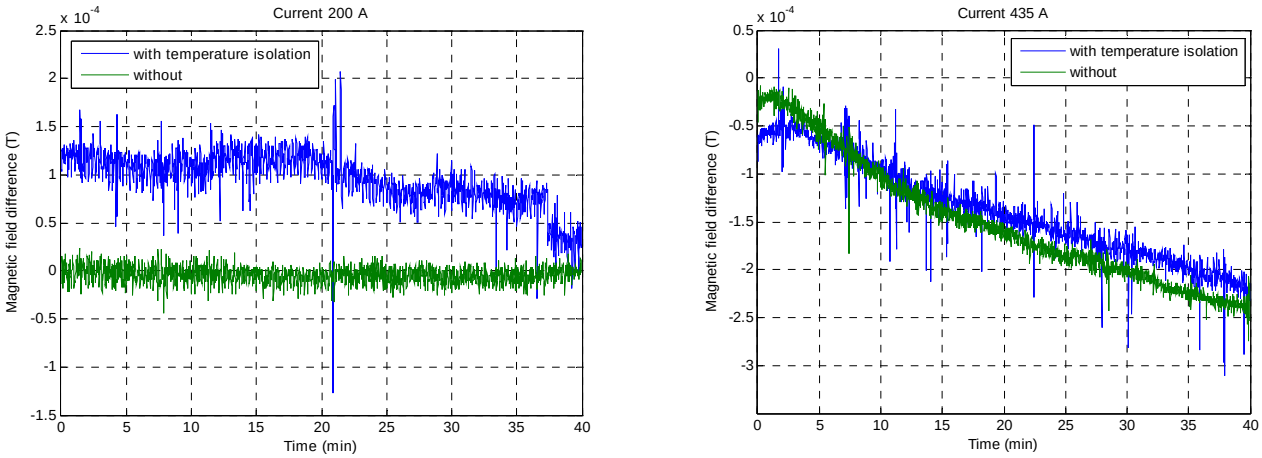

Figure 24 Change of magnetic field with time with and without thermal shield

4.4 Fine tuning of the first and second field integral

The final fine tuning of the first and second field integral was adjusted by using the first and last correctors only. Those correctors have the following responses:

- Current variation in coil 22 changes the first field integral: 0.1 A up -> first integral down by 150 G·cm. It does not influence the second field integral.
- Current variation in coil 1 changes the second field integral but also influences the first one: 0.1 A up -> second integral down by 70 kG·cm^2, first integral down by 60 G·cm.

4.5 3d field mapping

The undulator magnetic field tuning was done using on-axis measurements only. For some regimes, also 3d maps of the vertical field component were taken (x=-10,-5,0,5,10 mm, y=-5,0,5 mm). The results of mapping are presented in Figure 25 – Figure 30. The field integral variations are close to the limits of the measurement accuracy.

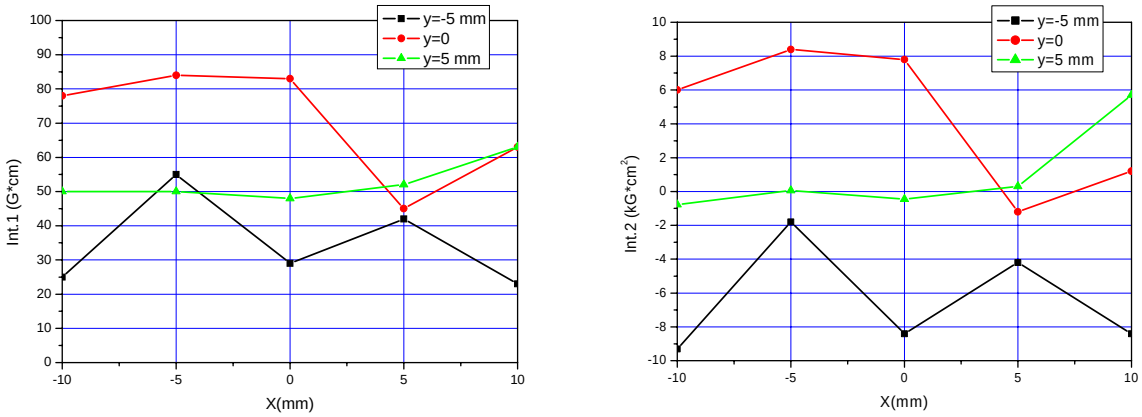

Figure 25 Field integrals at 50 A main coil excitation

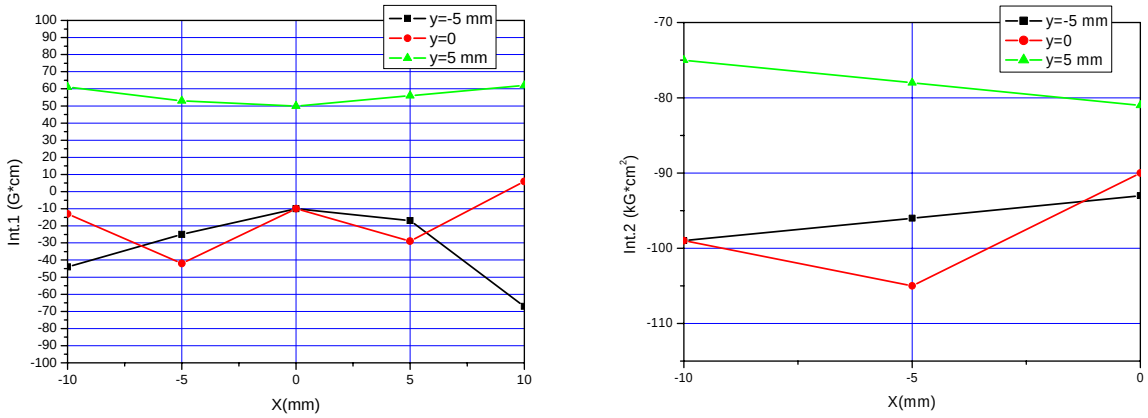

Figure 26 Field integrals at 123.2 A main coil excitation

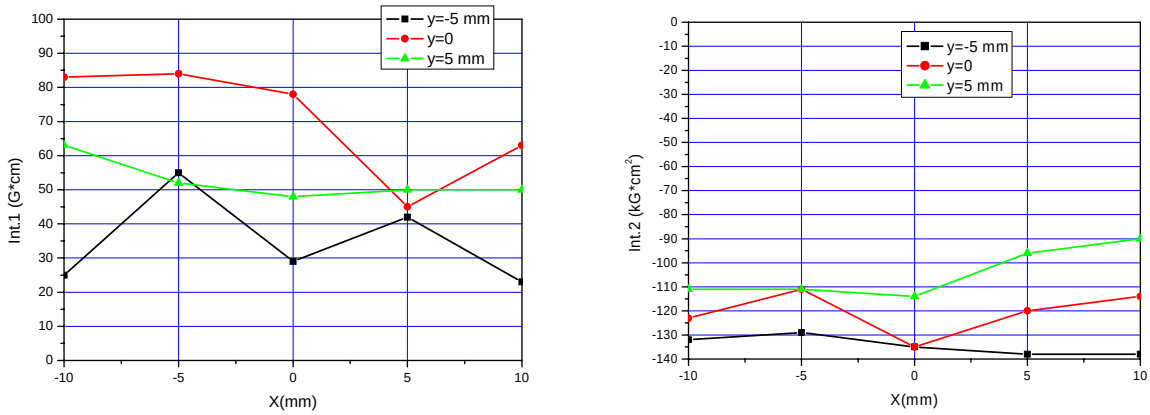

Figure 27 Field integrals at 200 A main coil excitation

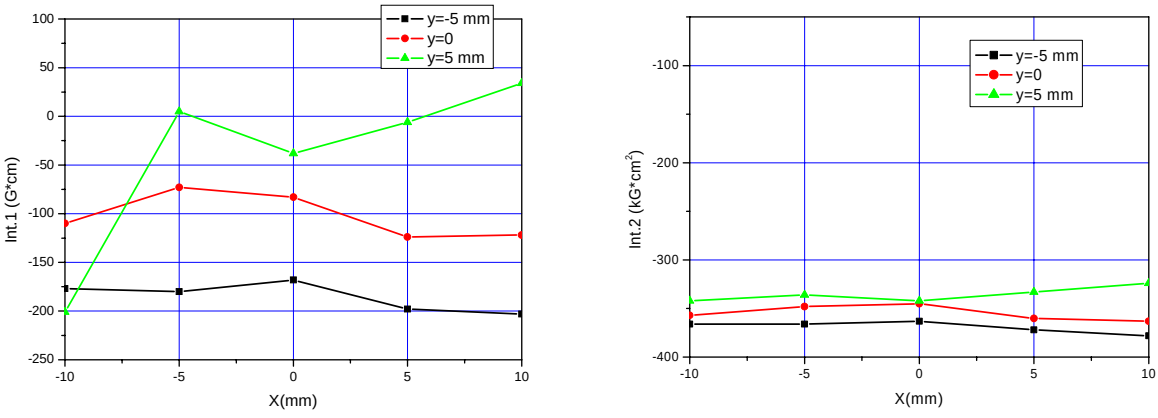

Figure 28 Field integrals at 300 A main coil excitation

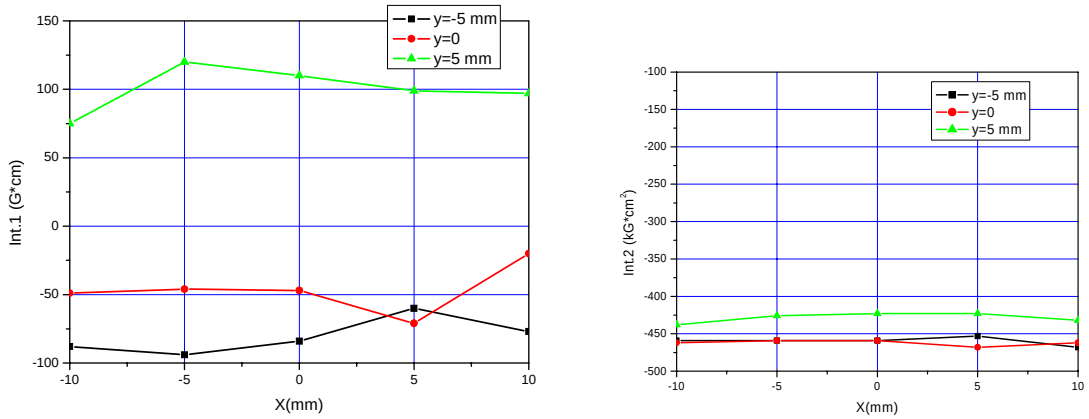

Figure 29 Field integrals at 340 A main coil excitation

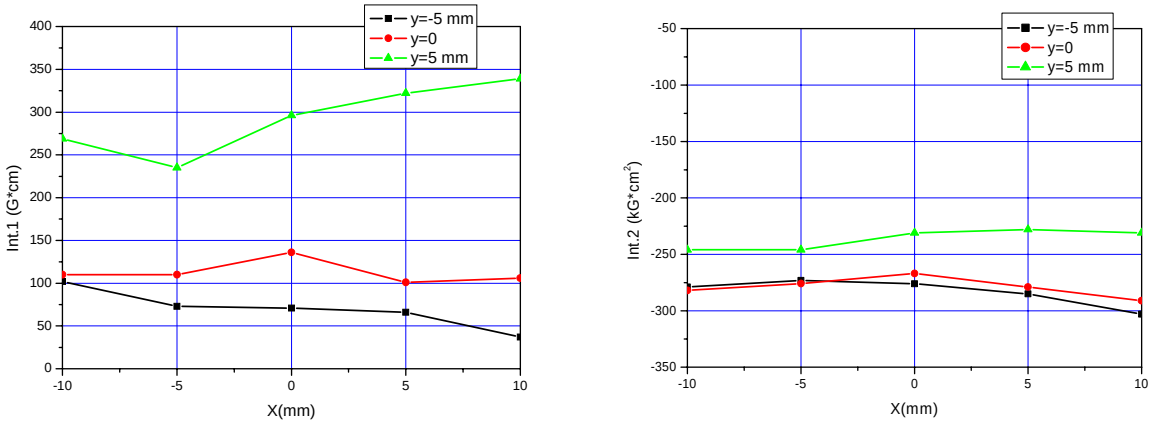

Figure 30 Field integrals at 435 A main coil excitation

4.6 Transverse field distributions

The results of the measurements of the undulator magnetic field in transverse direction for five pole pairs and three excitation currents are presented in Figure 31 - Figure 33 and compared for an excitation of 200 A in Figure 34.

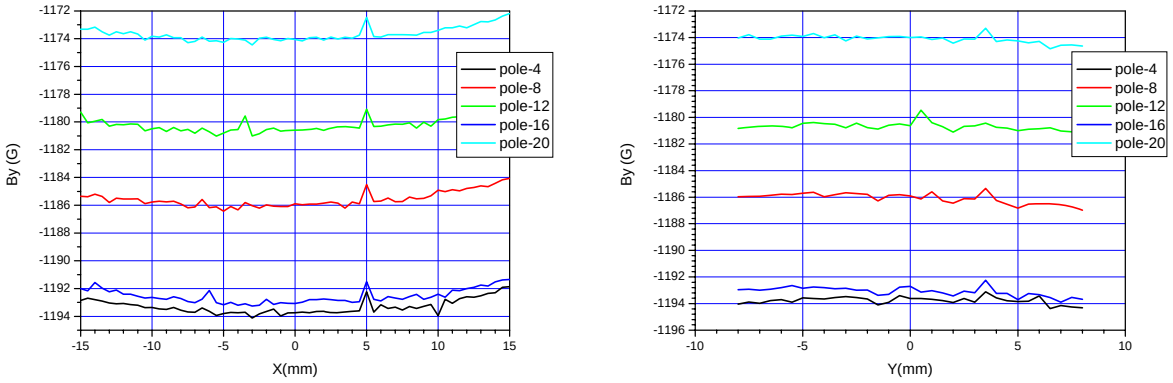

Figure 31 Horizontal and vertical field profiles at 30 A

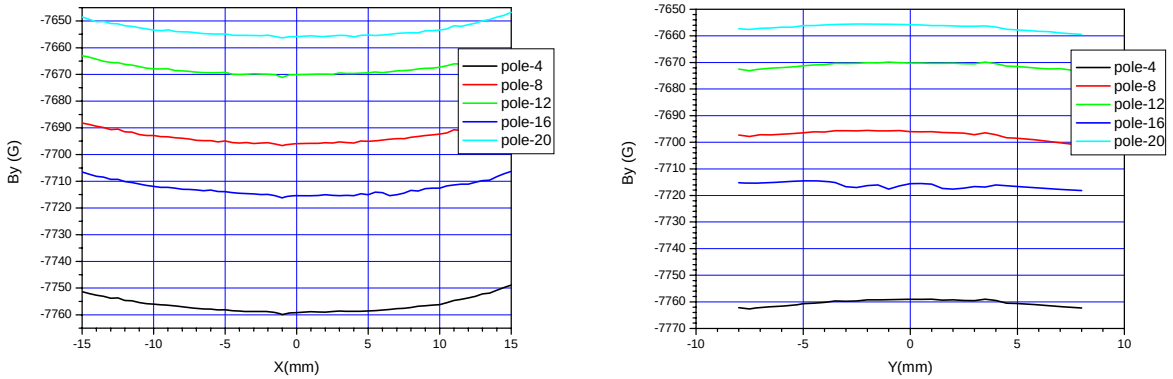

Figure 32 Horizontal and vertical field profiles at 200 A

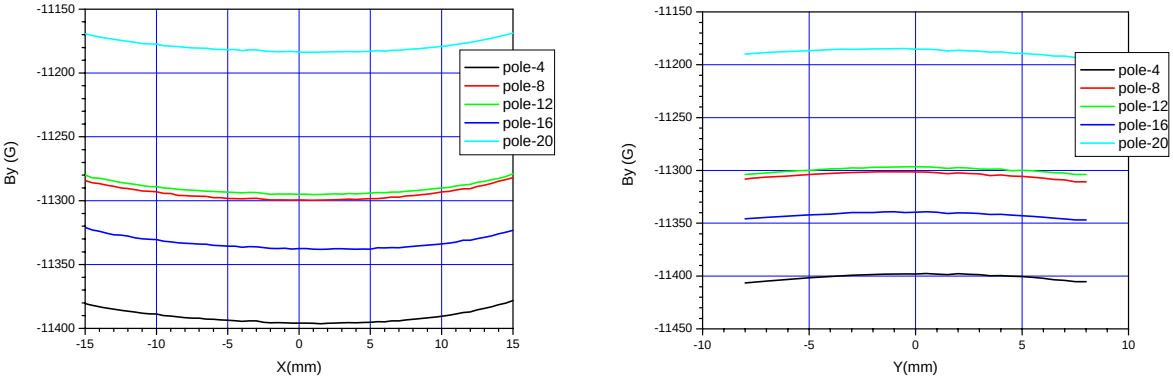

Figure 33 Horizontal and vertical field profiles at 435 A

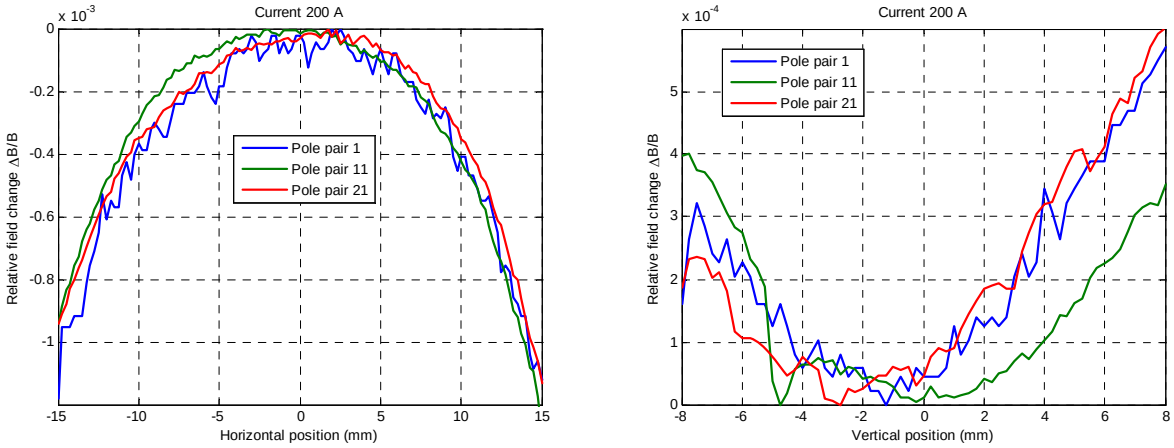

Figure 34 Transverse field profiles at 200 A excitation current

4.7 Temperature transients

The undulator consumes up to 110 kW electrical power at maximum excitation (252 V at 435 A). Operation will require frequent changes in the excitation current, therefore the time scales for transients, especially on the magnetic field integrals, is needed.

Figure 35 shows the rise and fall of the water temperature with time when ramping the current from 0 to 415 A (100 kW power) and back. Ramping of the power supply takes about 4 minutes. Time zero in the figure is not exactly coinciding with the start of the ramp. Within about 10 minutes, the water temperature has reached equilibrium. There is no further rise noticeable even when running for 24 hours. As the coils are in direct contact with the water, they also will have reached equilibrium after 10 minutes. The measured magnetic field itself does still change over a period of about 6 hours, as seen in Figure 36. The Hall probe was positioned centrally in pole pair 17, and the undulator powered with 435 A main coil current.

Both power supply and Hall probe have an accuracy of about 10^{-4}, consistent with the small fluctuations after 6 hours. The initial decrease of the field of the order of 5×10^{-4} is likely due to temperature effects of the undulator. A contribution from the power supply cannot be excluded, but it has significantly less thermal mass to provide such a long time constant. The Hall probe has a temperature coefficient of 1×10^{-5}/K and a zero drift of ±1 µT/K and, as the air in the open gap of the undulator cannot be heated significantly, will not contribute to this drift.

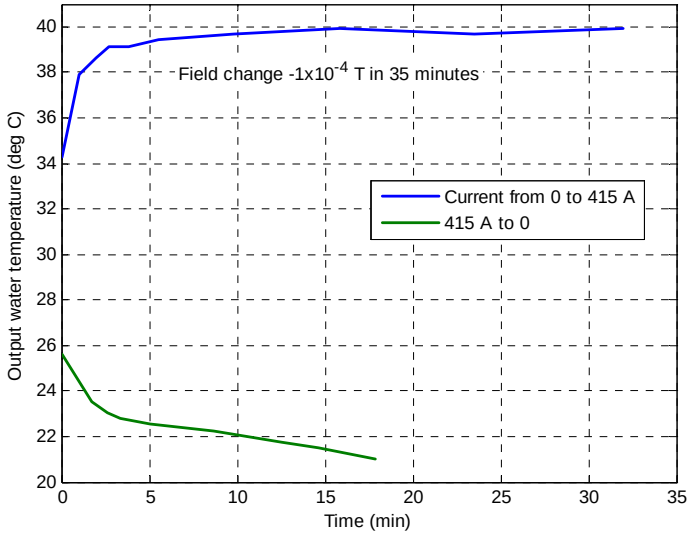

Figure 35 Change of water output temperature with time

To investigate temperature effects of the undulator, a Fluke Ti45 thermography camera was used[5]. As temperature changes are of concern here, and not absolute values, the emissivity value was left fixed at 0.95 (this value gives correct absolute temperatures for example for the rubber water pipes of the undulator). Figure 37 shows an example of such thermographic images. From a series of such measurement, the outside of the coils are found to be in equilibrium after about 30 minutes. The coils themselves are in good contact with the water, but the epoxy glue around them has bad heat conductivity, resulting in a longer time scale than the water itself.

The thermal coupling of the coils to the massive iron yoke and the support structure is weak and explains the 6 hour time constant found for the magnetic field.

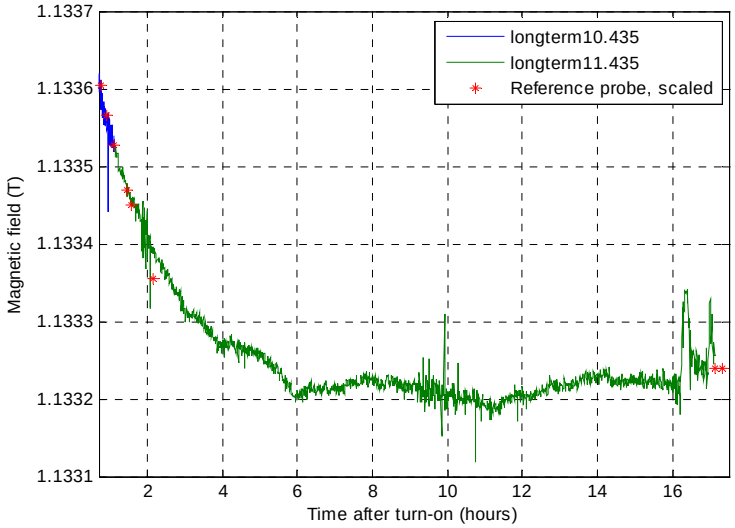

Figure 36 Magnetic field change at pole pair 17 at 435 A current.

[5] The camera has been provided and operated by H. Hirsemann, MEA2.

In Figure 38, thermographic images show details of the yoke and the support structure and how they heat up over a longer time. They were taken at the beginning and end of the long-term measurement of Figure 36.

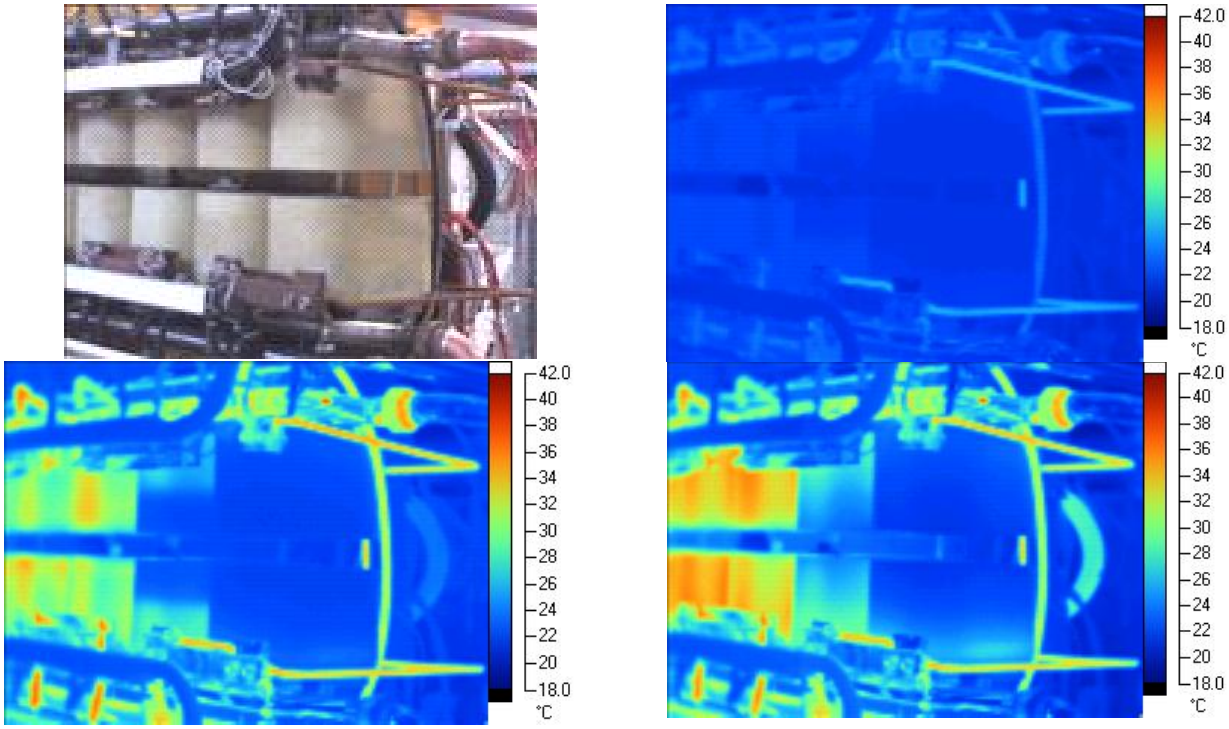

Figure 37 Thermographic images before switching on with 435 A, 10 minutes later and 60 minutes later (clockwise). Emissivity 0.95.

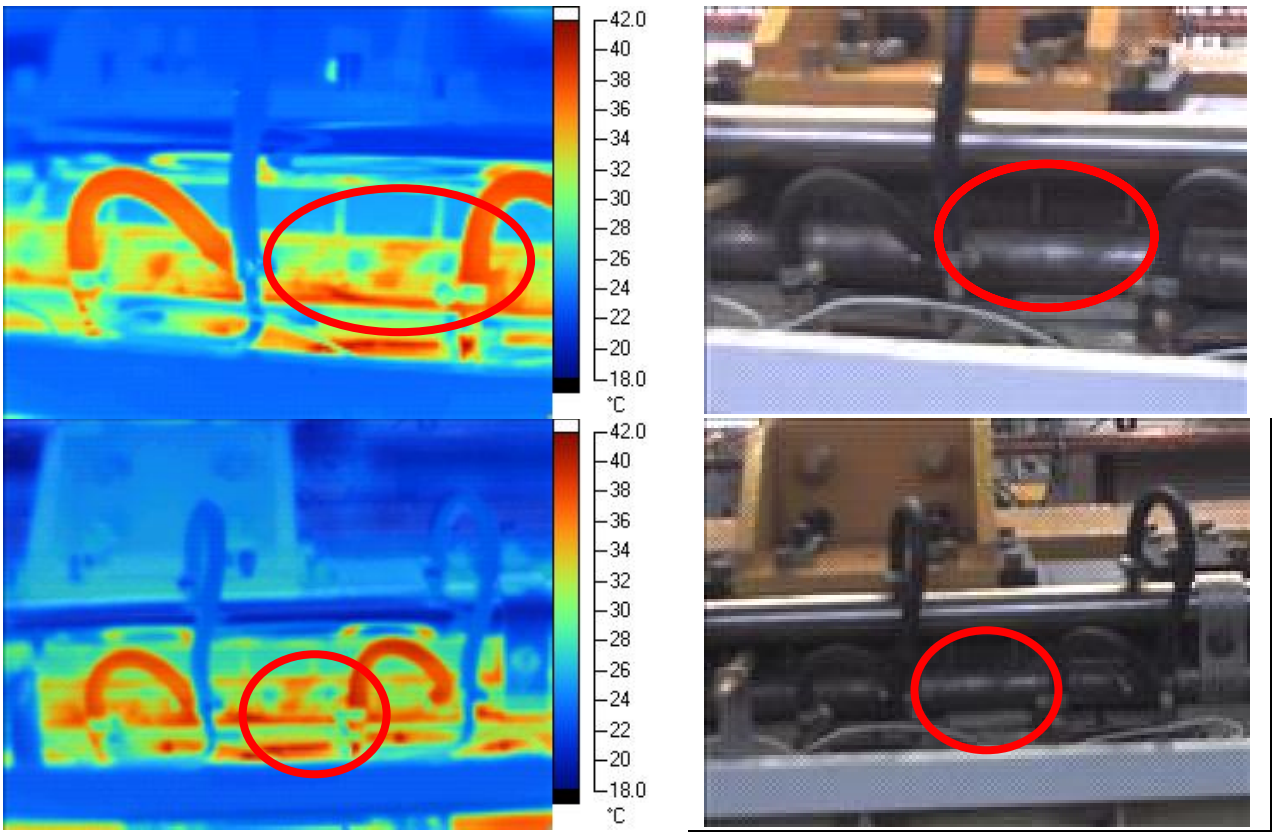

Figure 38 Thermogaphic images 1 hour and 17 hours after switching on with 435 A.

Due to the special winding of the end coils, peculiar heating and cooling patterns can be observed, an example of which is shown in Figure 39. Only the part of the epoxy glue that has copper windings underneath is cooled relatively quickly after switching off the current.

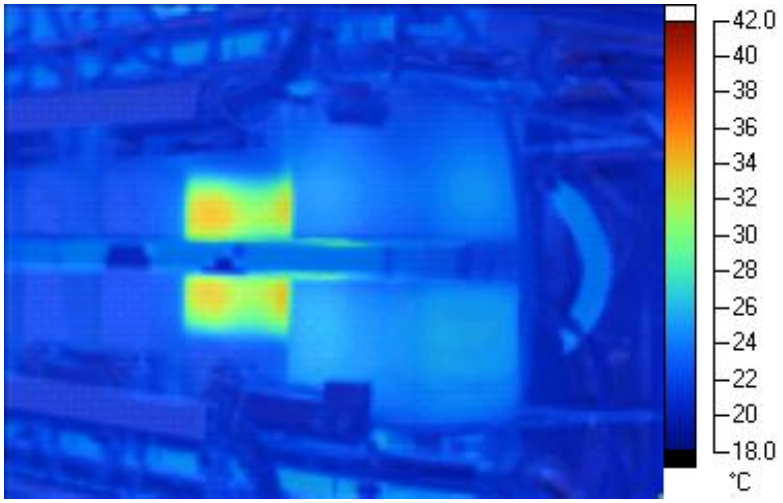

Figure 39 Thermographic image 30 minutes after switching off, following an overnight running at 435 A.

The long-term undulator magnetic field-integral variation was studied during a 27 hour run at maximum excitation current of 435 A. Each hour during the day magnetic field measurements were done. The results are shown in Figure 40. Although the magnetic field itself changes over a period of several hours, the field integrals are immediately stable. This finding can be attributed to thermal expansion of the yoke: the field changes due to gap changes, but the field integral is compensated by a similar longitudinal expansion.

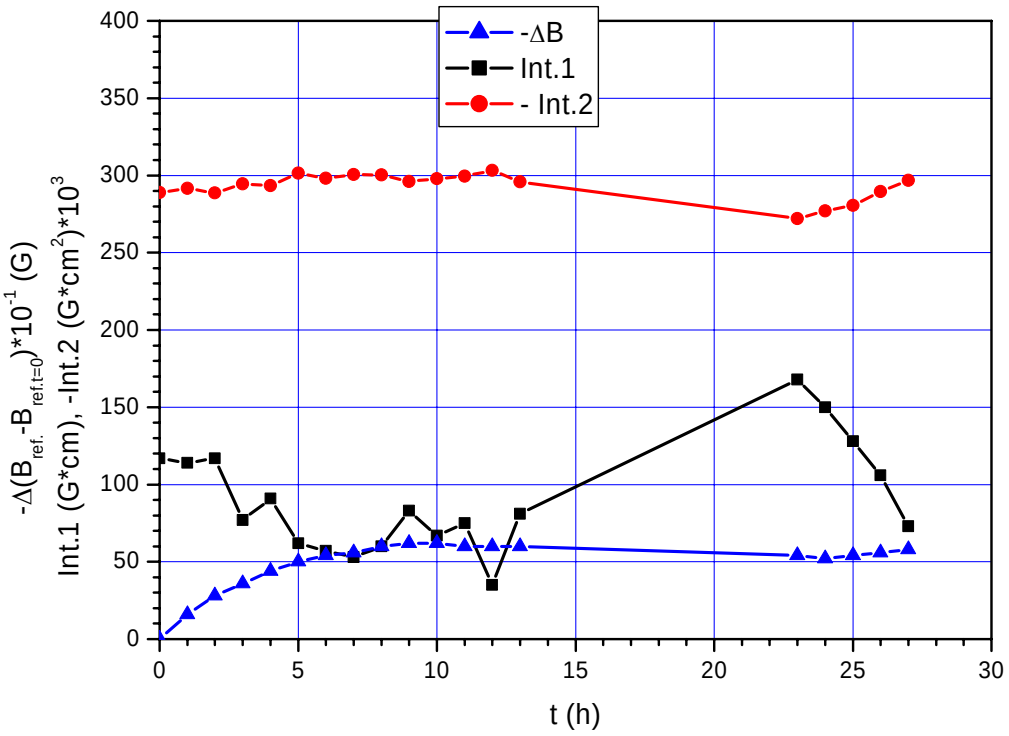

Figure 40 Data for the long test run of the undulator

5 Undulator operation

This section summarizes the results from the magnetic tuning that are relevant for actual operation of the undulator. It does not contain information about the operation within the context of the FLASH accelerator, as this will require machine specific settings that will be determined only during dedicated commissioning shifts and will be reported separately.

5.1 Corrector coil settings

The basic result of the undulator tuning is the determination of correct corrector coil settings for all main coil excitations. These settings are listed in Table 2, together with the measured first and second field integral over the undulator length (integrals determined over 5 m). The file name refers to the data file that contains the actual longitudinal magnetic field profile as obtained with the Hall probe. The currents are also graphically shown in Figure 41.

Table 2 Parameters for the basic undulator set points

I_{main} (A)	File name	P12 left(A)	P3 right(A)	P1 (A)	P22 (A)	P2 (A)	P21 (A)	Int.1 (G·cm)	Int.2 (kG·cm^2)	K
0	D-402	0	0	0.53	0.7	0	0	23	-18	0.356
2	D-403	-0.01	-0.45	0.0	0.18	0.12	-0.18	-63	-10.5	0.455
5	D-404	-0.03	-0.4	-0.05	0.45	0.29	-0.46	-12	-8.1	0.846
12	D-406	-0.072	-0.45	-0.30	1.08	0.68	-1.1	-88	12.9	1.88
20	D-411	-0.12	-0.134	-0.27	1.3	1.14	-1.07	-34	-1.5	3.08
30	D-414	-0.18	-0.2	-0.7	1.65	1.7	-1.6	-47	-3.9	4.58
50	D-417	-0.3	-0.32	-1.0	1.95	2.4	-2.4	-58	8.7	7.63
78	D-419	-0.4	-0.43	-1.4	2	3.4	-3.1	-129	-69	11.9
90	D-422	-0.5	-0.5	-1.6	2.1	4	-3.7	-73	-129	13.7
123.2	D-424	-0.67	-0.67	-2.6	3.1	5.4	-5.2	-86	-126	18.8
170	D-437	-0.9	-0.9	-2.7	3.0	6	-5.7	-81	-122	25.8
200	D-440	-1	-1	-3.2	3.8	6.3	-6	-52	-183	29.6
230	D-442	-1.1	-1.1	-2.1	3.2	4.6	-4.6	-52	-122	32.7
260	D-444	-1.2	-1.2	-1.7	3.0	3	-3.1	23	-249	35.2
275	D-446	-1.2	-1.2	-1.5	3.1	2.1	-2.4	52	-141	36.2
300	D-447	-1.1	-1.1	-0.5	2.6	0.1	-0.3	-151	-354	37.9
332.7	D-449	-1	-1	0.55	1.5	-2.5	2.6	-58	-405	39.6
340	D-450	-1	-1	1.2	1.2	-3.4	3.3	-146	-462	39.9
380	D-451	-1.5	-1.2	2.7	0	-7	6.8	-49	-381	41.6
390	D-453	-1.6	-1.2	3.2	-0.6	-8	7.8	94	-378	41.9
420	D-455	-1.6	-1.2	2.8	0.4	-8.4	7.8	-46	-345	42.0
435	D-457	-1.6	-1.2	2.5	0.7	-8.4	7.8	10	-321	43.5

The K value is calculated from the first harmonic wavelength that was obtained from numerical simulation of the on-axis spectrum according to $\lambda = \frac{\lambda_u}{2\gamma^2}\left(1+\frac{K^2}{2}\right)$.

Corrector settings for main excitations at other values are obtained by linear interpolation. The full corrector listing in steps of 1 A main coil excitation is given in Appendix C.

The power supply designation in the FLASH control system is U6EXP for the main power supply, and U6PxEXP for the six correctors, where x designates the pole pair or first pole pair on which the respective power supply acts.

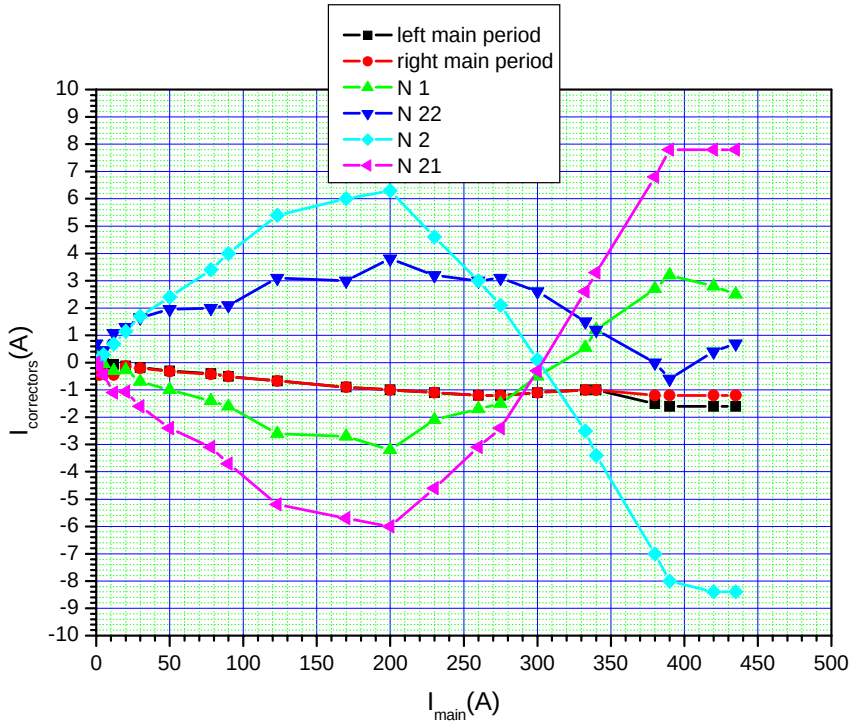

Figure 41 Corrector coil settings

5.2 Procedure for regime change, cycling procedure

An important goal of the magnetic measurements was to achieve good reproducibility of the undulator tuning with respect to the field integrals. The cycling procedure of the undulator to give well defined initial conditions consists of exciting the main coil with 0 A, then 435 A, then 0 A again. All correctors should be at 0 A (or off). The coils are then set to the desired value in the following order:

1. Main coils
2. U6P12EXP (left)
3. U6P3EXP (right)
4. U6P1EXP
5. U6P22EXP
6. U6P2EXP
7. U6P21EXP

To change the main coil excitation, first set the correction coil currents to zero in the opposite order. If the new main coil excitation is higher than the current, set the new value directly. If it is lower, first go to 435 A, then to 0 A, then to the new target value. The corrector are then switched on in the order given above.

Results on the reproducibility of first and second field integral are shown Figure 42 and Figure 43.

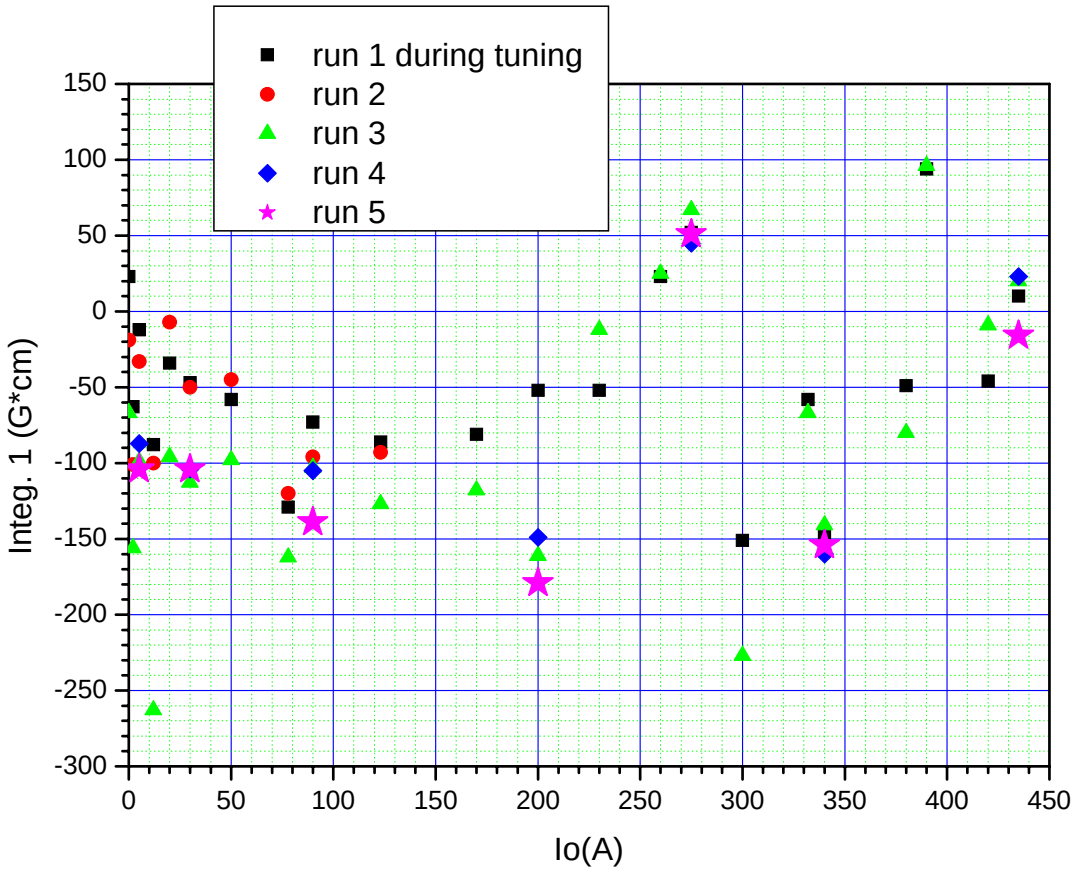

Figure 42 Reproducibility of first field integral

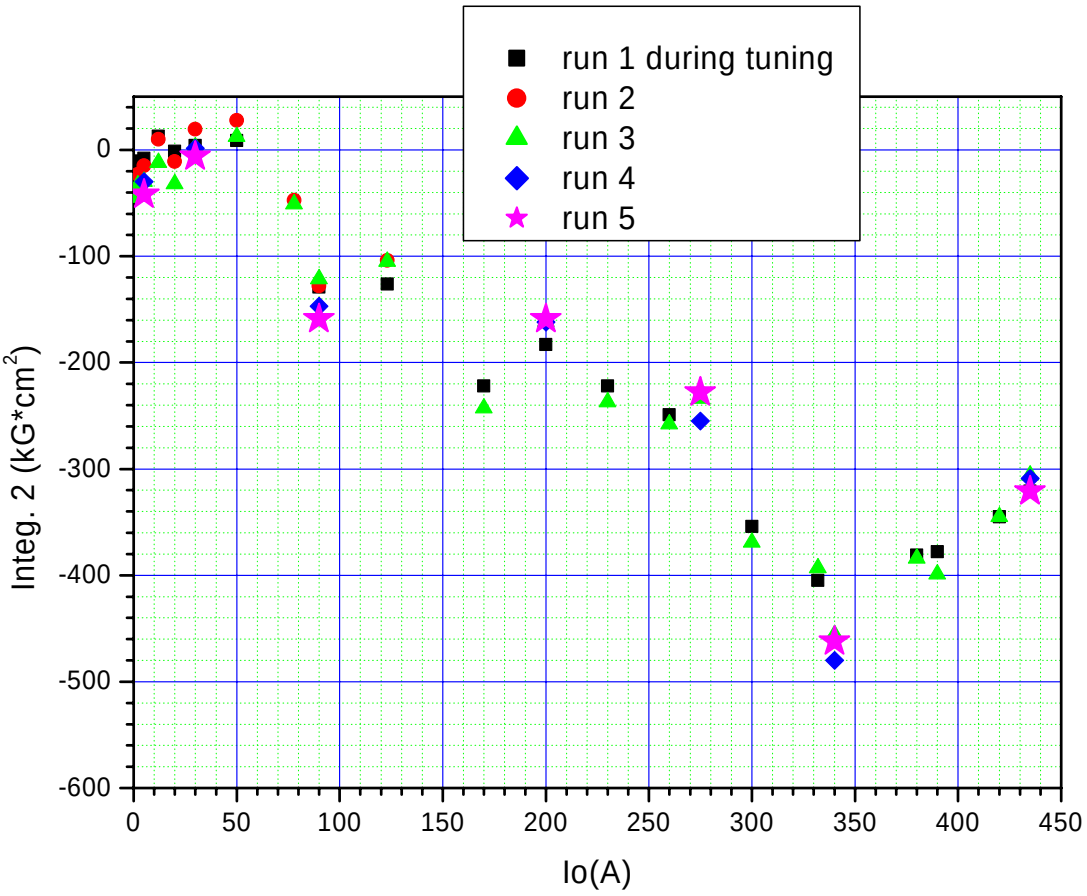

Figure 43 Reproducibility of second field integral

5.3 Degaussing procedure

The objective of the degaussing procedure is to minimize the remnant magnetic field. The excitation main coil current in Amps for the degaussing procedure are as follows (moving from one current to the next at the slew rate of the power supply):

+400, -400, +200, -100, +50, -40, +30, -20, +15, -13, +11, -9, +7, -5, +4, -3, +2, -1, +0.5, -0.25, 0

The distribution of the remnant magnetic field before and after degaussing is shown in Figure 44. The maximum value of the remnant field was decreased to about 3 G, though the second field integral has approximately the same behavior as before degaussing (Figure 45) due to the remaining DC field component.

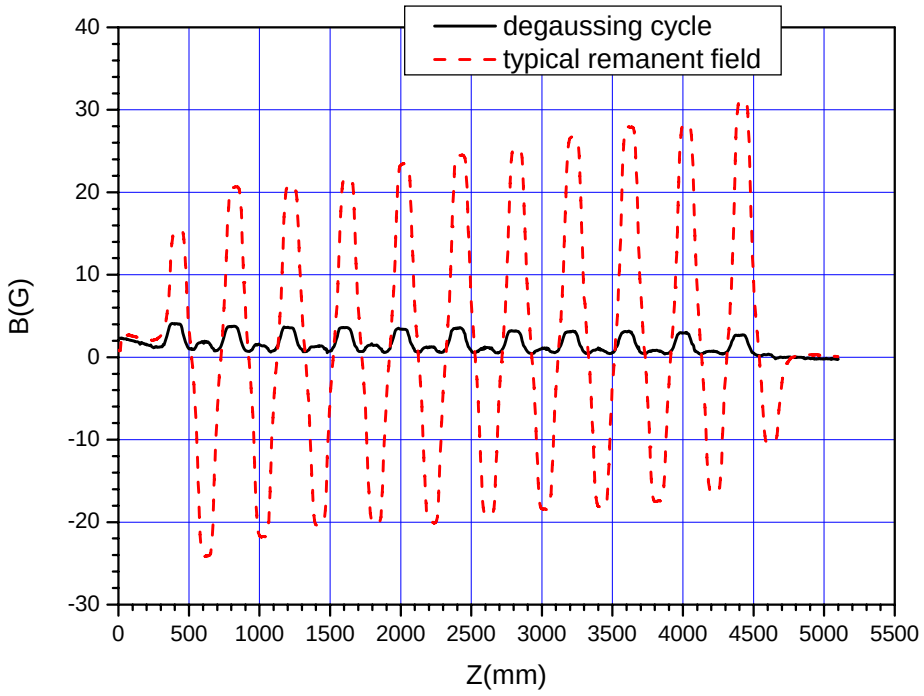

Figure 44 Typical remnant magnetic field and the field after degaussing cycle

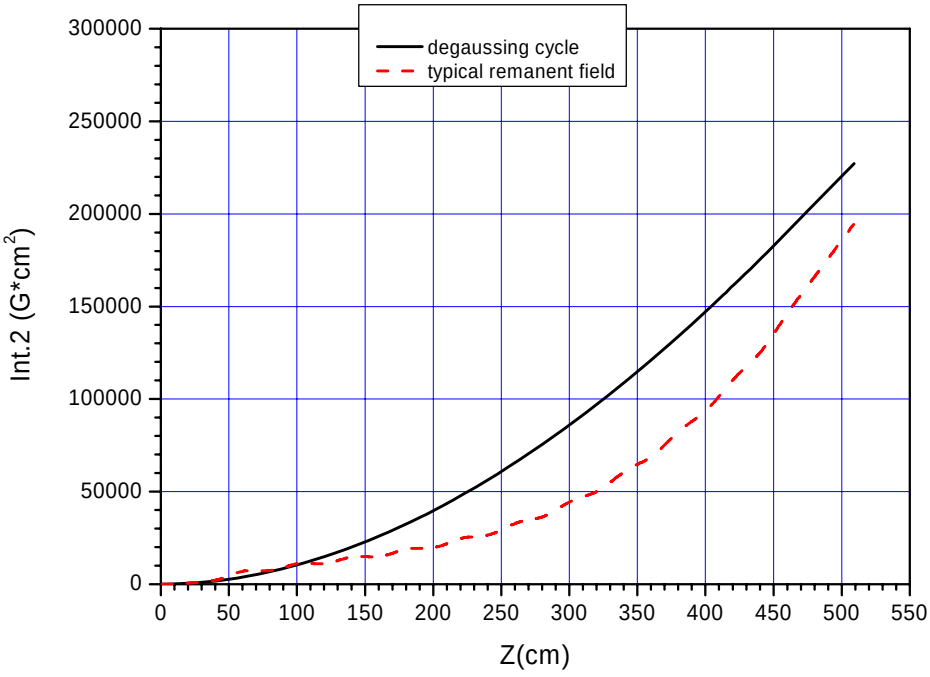

Figure 45 Second field integral of the remnant field before and after degaussing

A Referencing of tuning circuitry

As the main coil correction coils are set via adjustable resistors and a number of switches at the back side of the undulator, referencing is necessary in case they are changed by accident or because a replacement of a broken part is necessary.

To this end, the current of the main coil correction coils (U6P3EXP and U6P12EXP) is set to -1 A, and the voltage measured the voltage between contacts N6 (ground) and N3 (signal). If necessary, the potentiometers should be adjusted to get the voltages listed below to better than 100 mV. The switch positions are given in brackets. The mail coil current should be at 200 A. In small print are the results obtained just prior to installation of the undulator in the FLASH tunnel, both at 0 (left) and 200 A (right) main coil current.

R1	1.27 V (up/down) 1.28/1.28	R7	3.05 V (up/down) 3.06/3.08	R13	-2.1 V (up/up) -2.06/-2.07
R2	2.1 V (up/down) 2.07/2.07	R8	0 V (down/down) 0.01/0.01	R14	-1.6 V (up/up) -1.59/n/a
R3	2.1 V (up/down) 2.07/2.08	R9	-2.7 V (up/up) -2.66/-2.67	R15	-5.9 V (up/up) -5.84/-5.91
R4	2.53 V (up/down) 2.50/2.51	R10	0 V (down/down) 0.02/0.02	R16	-2.17 V (up/up) -2.16/-2.17
R5	-0.59 V (up/up) -0.58/-0.58	R11	-3.48 V (up/up) -3.39/-3.41	R17	1.74 V (up/down) 1.72/1.73
R6	-0.51 V (up/up) -0.54/-0.54	R12	-4 V (up/up) -3.93/-3.96	R18	-0.93 V (up/up) -0.93/-0.93

At 200 A, the measured voltages are on average about 0.5% higher than at zero current, indicating a negligible influence of temperature on the referencing.

B Coils resistivities

The voltage over each main coil was measured at 200 A excitation current, see Figure 46. They translate into resistances as follows:

Pole #	1	2	3	4	5	6	7	8	9	10	11
R (mΩ)	1.76	1.73	8.05	8.23	14.57	14.47	14.49	15.39	14.25	14.72	14.90
	12	13	14	15	16	17	18	19	20	21	22
	14.28	14.72	14.21	14.48	14.86	14.38	14.49	15.05	14.27	14.33	14.79
	23	24	25	26	27	28	29	30	31	32	33
	14.45	14.71	14.75	15.01	14.39	14.42	14.62	14.65	14.75	14.72	14.90
	34	35	36	37	38	39	40	41	42	43	44
	14.69	14.40	14.67	14.22	14.30	14.36	14.41	7.99	8.07	1.73	1.62

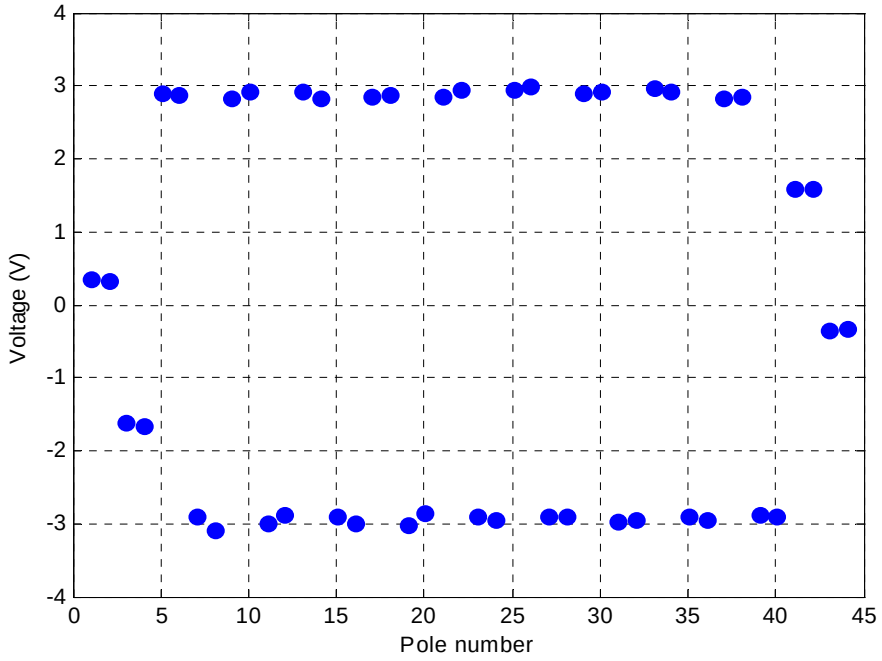

Figure 46 Voltage over all 44 coils at 200 A current

The edge corrector coil resistances have the following measured resistances (the deviation of sum from individual values indicates the measurement accuracy) :

Pole #	1	2	3	4	41	42	43	44	1+2	3+4	41+42	43+44
R (Ω)	0.52	0.55	0.55	0.56	0.55	0.53	0.55	0.52	1.06	1.05	1.11	1.07

C Magnetization data for pole-pair 11

The magnetic field at the centre of pole pair 11 has been measured with high resolution as a function of main coil excitation. The correctors were set for each value as required by the tuning.

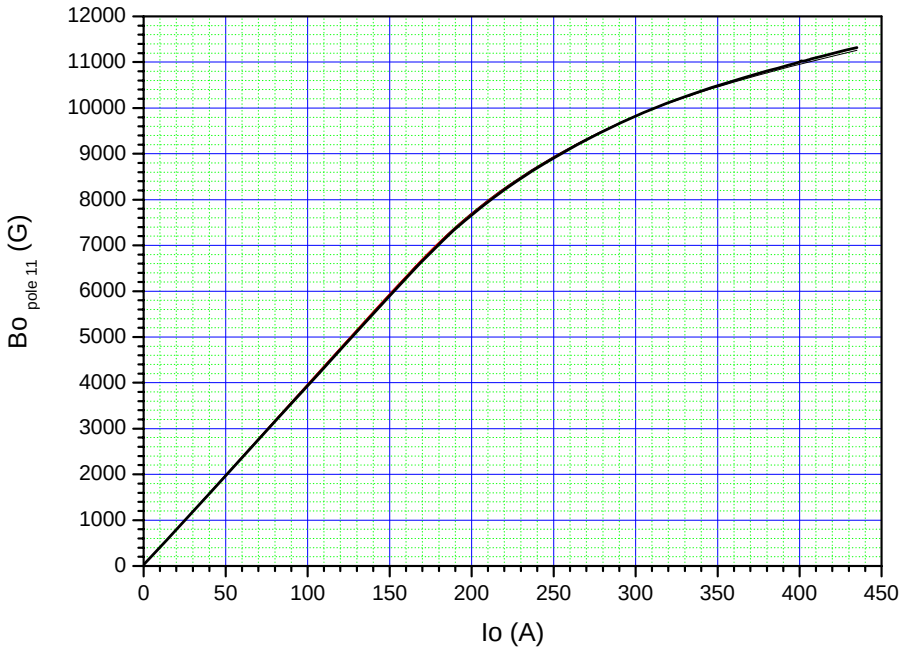

Figure 47 Magnetization curve for pole 11

Io (A)	B (G)
0	26.34
1	67.23
2	107.41
3	143.32
4	180.51
5	217.76
6	256.02
7	296.92
8	335.43
9	372.67
10	411.54
11	449.31
12	487.54
13	525.83
14	566.4

15	603.15
16	641.59
17	678.61
18	717.66
19	755.83
20	794.09
21	833.39
22	872.26
23	910.6
24	950.01
25	989.55
26	1027.97
27	1067.11
28	1106.14
29	1144.99
30	1184.26
31	1223.16

32	1262.38
33	1301.46
34	1340.61
35	1380.11
36	1419.1
37	1458.36
38	1497.31
39	1536.63
40	1575.8
41	1614.82
42	1654.2
43	1693.47
44	1732.59
45	1771.65
46	1811.27
47	1850.35
48	1889.5

49	1929.33
50	1968.56
51	2007.75
52	2047.83
53	2087.26
54	2126.48
55	2166.24
56	2205.28
57	2244.73
58	2283.9
59	2323.55
60	2362.77
61	2402.36
62	2442.01
63	2481.44
64	2520.99
65	2560.31

66	2600.03
67	2639.44
68	2679.02
69	2718.21
70	2760.84
71	2798.7
72	2838.08
73	2877
74	2916.27
75	2955.72
76	2995.29
77	3035.09
78	3073.89
79	3111.26
80	3151.67
81	3190.93
82	3230.47
83	3269.88
84	3308.88
85	3348.09
86	3387.48
87	3426.3
88	3465.4
89	3504.37
90	3543.96
91	3583.44
92	3627.94
93	3662.18
94	3701.91
95	3740.76
96	3780.24
97	3819.55
98	3859.12
99	3898.28
100	3937.66
101	3977.02
102	4016.55
103	4055.78
104	4095.11
105	4135.37
106	4174.11
107	4213.05
108	4252.32
109	4291.59
110	4330.84
111	4370.37
112	4409.83
113	4448.82
114	4488.46
115	4527.31
116	4566.68
117	4606.33
118	4645.18
119	4684.9
120	4724.07
121	4763.17

122	4802.71
123.2	4849.32
124	4881.75
125	4920.33
126	4959.51
127	4998.78
128	5037.55
129	5076.87
130	5116.81
131	5155.2
132	5194.99
133	5233.96
134	5273.05
135	5312.1
136	5351.32
137	5390.4
138	5429.58
139	5468.29
140	5507.48
141	5546.49
142	5585.56
143	5624.56
144	5663.49
145	5702.28
146	5741.58
147	5787.19
148	5819.06
149	5857.93
150	5896.73
151	5935.36
152	5974.48
153	6013.18
154	6051.58
155	6089.89
156	6128.24
157	6167.52
158	6205.43
159	6243.37
160	6282.15
161	6320.21
162	6358.22
163	6397.01
164	6434.19
165	6473.12
166	6509.27
167	6546.85
168	6584.13
169	6621.23
170	6658.4
171	6695.52
172	6732.08
173	6768.77
174	6805.38
175	6842.49
176	6877.53
177	6913.28

178	6949.13
179	6984.17
180	7018.58
181	7053.53
182	7087.92
183	7122.56
184	7156.63
185	7189.83
186	7223.48
187	7256.4
188	7296.14
189	7321.94
190	7354.37
191	7386.66
192	7418.11
193	7449.11
194	7481.19
195	7512.18
196	7542.9
197	7573.62
198	7603.7
199	7633.5
200	7662.97
201	7692.8
202	7722.57
203	7751.16
204	7780.2
205	7808.95
206	7837.05
207	7865.27
208	7893.08
209	7921.17
210	7948.75
211	7975.98
212	8002.17
213	8029.15
214	8055.66
215	8082.16
216	8108.53
217	8134.93
218	8161
219	8186.84
220	8217.99
221	8240.11
222	8265.28
223	8290.29
224	8315.02
225	8339.67
226	8364.12
227	8388.48
228	8412.88
229	8436.55
230	8460.59
231	8484.34
232	8508.12
233	8531.75

234	8554.62
235	8577.65
236	8600.82
237	8624.02
238	8646
239	8668.79
240	8691.17
241	8712.55
242	8734.98
243	8756.66
244	8778.61
245	8800.38
246	8822.07
247	8843.31
248	8865.04
249	8886.39
250	8907.2
251	8928.36
252	8948.95
253	8969.72
254	8990.26
255	9010.74
256	9030.79
257	9051.5
258	9071.28
259	9091.48
260	9111.09
261	9131
262	9151.09
263	9169.47
264	9188.88
265	9209.54
266	9228.46
267	9247.74
268	9267.06
269	9285.73
270	9304.64
271	9323.61
272	9342.01
273	9360.4
274	9379.09
275	9397.45
276	9415.92
277	9433.86
278	9452.15
279	9470.14
280	9487.97
281	9505.9
282	9523.28
283	9540.99
284	9558.72
285	9576.09
286	9593.25
287	9610.32
288	9627.47
289	9644.13

290	9661.32
291	9677.89
292	9694.55
293	9711.11
294	9727.66
295	9744.02
296	9760.25
297	9776.8
298	9793.05
299	9808.9
300	9822.48
301	9840.3
302	9855.69
303	9871.13
304	9886.57
305	9901.3
306	9916.75
307	9931.72
308	9946.85
309	9961.17
310	9975.55
311	9990.33
312	10004.85
313	10019.32
314	10033.67
315	10047.49
316	10061.37
317	10075.69
318	10089.55
319	10103.21
320	10116.85
321	10130.62
322	10144.02
323	10157.07
324	10170.12
325	10183.48
326	10196.57
327	10206.93
328	10220.02
329	10235.23
330	10247.76
331	10260.5
332.7	10273.24
333	10281.6
334	10297.85
335	10310.08
336	10322.5
337	10334.66

338	10346.67
339	10358.7
340	10371.06
341	10382.77
342	10394.37
343	10405.82
344	10417.56
345	10429.04
346	10440.42
347	10453.75
348	10465.19
349	10476.22
350	10487.54
351	10498.37
352	10509.59
353	10520.89
354	10531.25
355	10542.17
356	10553.56
357	10564.34
358	10575.2
359	10585.55
360	10596.81
361	10607.69
362	10618.2
363	10628.56
364	10636.28
365	10649.67
366	10660.11
367	10670.66
368	10681.24
369	10691.74
370	10702.01
371	10712.44
372	10722.97
373	10733.09
374	10743.69
375	10753.57
376	10763.83
377	10773.85
378	10784.12
379	10793.88
380	10804.36
381	10814.16
382	10824.38
383	10834.3
384	10844.19
385	10854.27

386	10864.11
387	10873.99
388	10883.61
389	10893.83
390	10903.38
391	10913.3
392	10923.66
393	10933.17
394	10943.23
395	10952.76
396	10962.63
397	10972.17
398	10982.05
399	10991.55
400	11001.08
401	11031.44
402	11020.85
403	11030.21
404	11039.63
405	11049.14
406	11058.42
407	11068.1
408	11077.58
409	11087.1
410	11096.36
411	11105.62
412	11115.25
413	11124.68
414	11133.77
415	11142.97
416	11152.27
417	11161.59
418	11170.68
419	11179.34
420	11189.04
421	11198.12
422	11207.01
423	11216.22
424	11225.08
425	11234.13
426	11242.9
427	11252.2
428	11260.86
429	11269.68
430	11278.7
431	11287.36
432	11295.99
433	11305.15

434	11313.65
435	11322.32

D Magnetic field integrals

The collection of first field integrals along the regular undulator periods is presented in Figure 48. The list of the first and the second integral values at the undulator output for the tuning settings is in Table 2. The second field integrals for all tuning settings are plotted below.

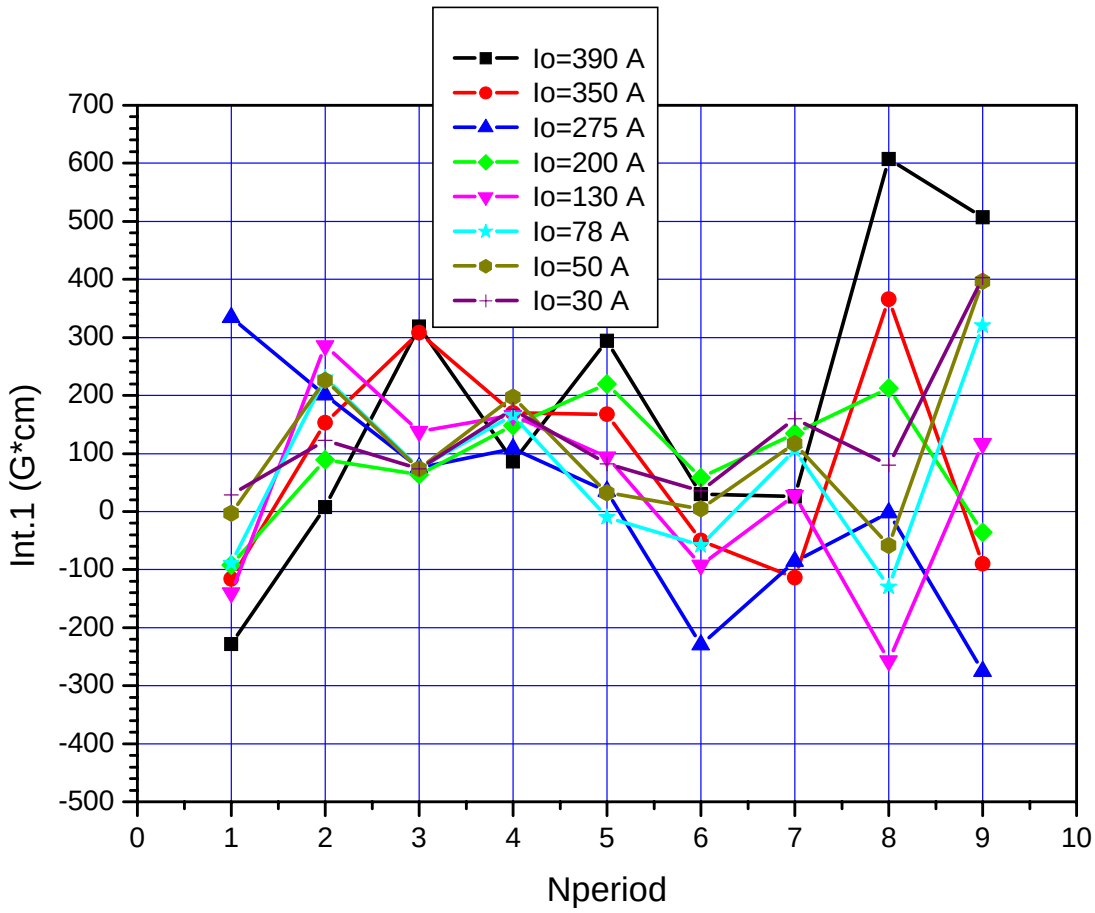

Figure 48 Magnetic field first integral for the undulator regular periods

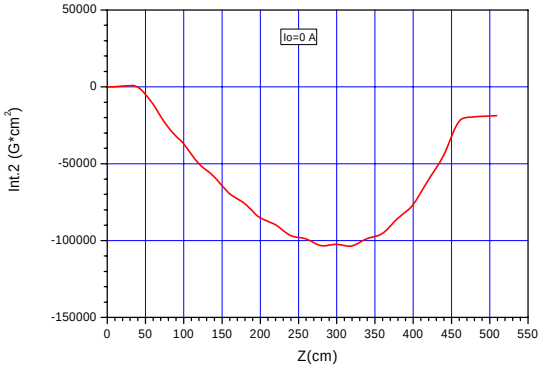
Io=0 A
Int.2 (G*cm²)
Z(cm)

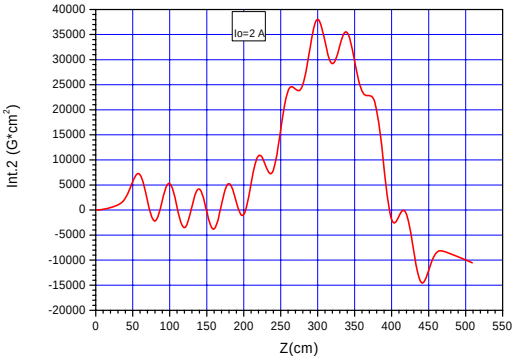
Io=2 A
Int.2 (G*cm²)
Z(cm)

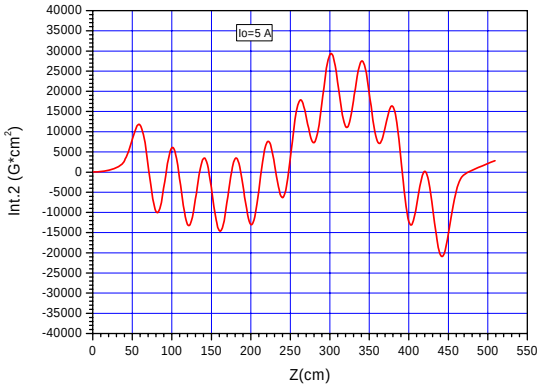
Io=5 A
Int.2 (G*cm²)
Z(cm)

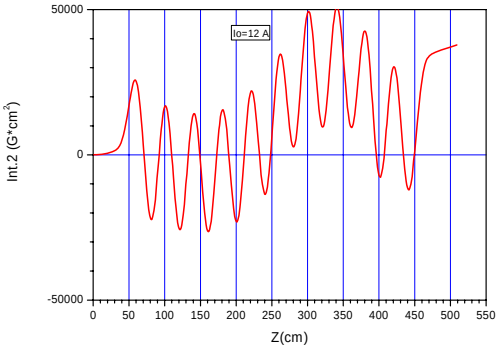
Io=12 A
Int.2 (G*cm²)
Z(cm)

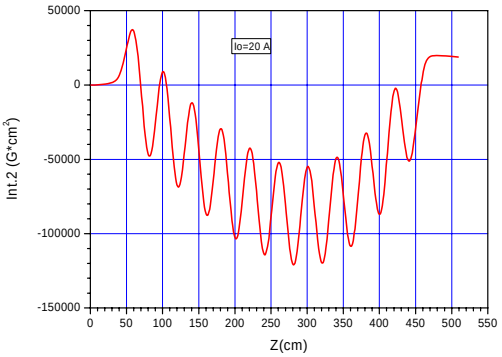
Io=20 A
Int.2 (G*cm²)
Z(cm)

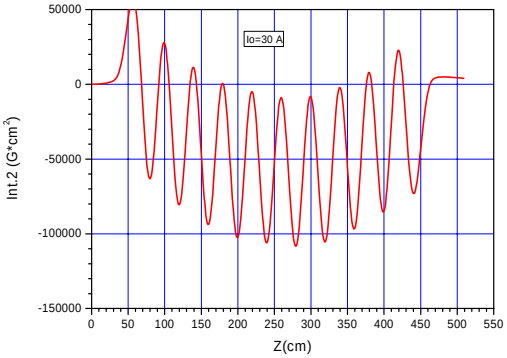
Io=30 A
Int.2 (G*cm²)
Z(cm)

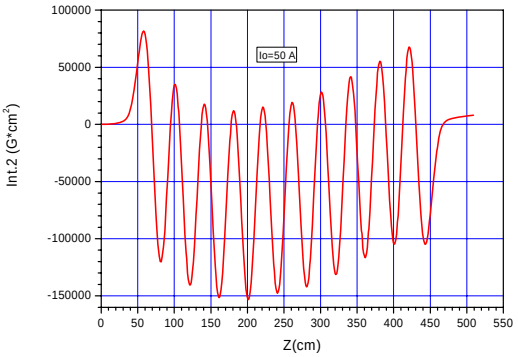
Io=50 A
Int.2 (G*cm²)
Z(cm)

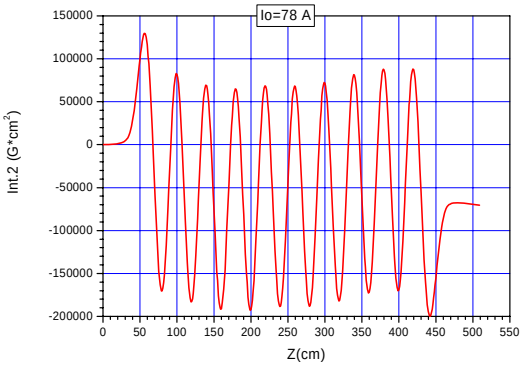
Io=78 A
Int.2 (G*cm²)
Z(cm)

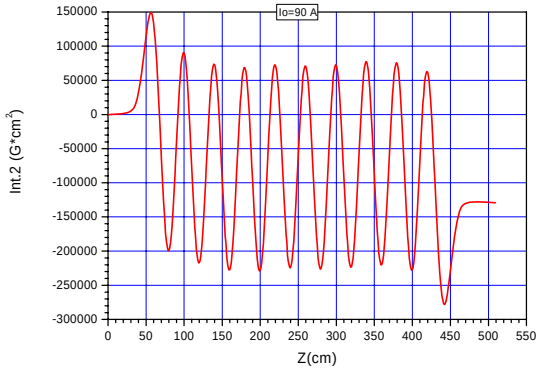
Io=90 A
Int.2 (G*cm²)
Z(cm)

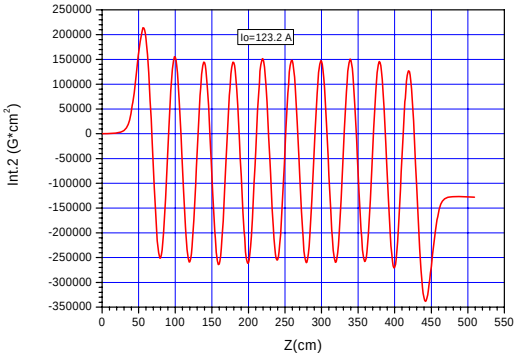
Io=123.2 A
Int.2 (G*cm²)
Z(cm)

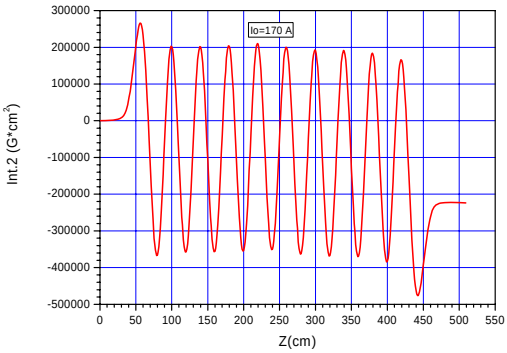
Io=170 A
Int.2 (G*cm²)
Z(cm)

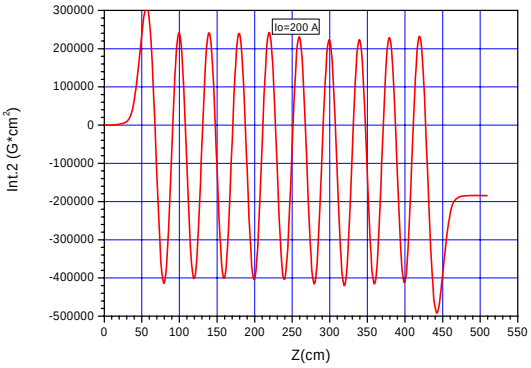
Io=200 A
Int.2 (G*cm²)
Z(cm)

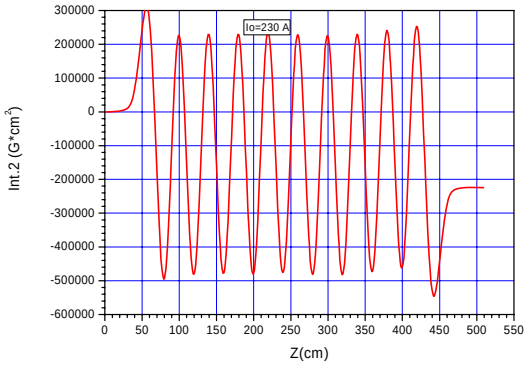
Io=230 A
Int.2 (G*cm²)
Z(cm)

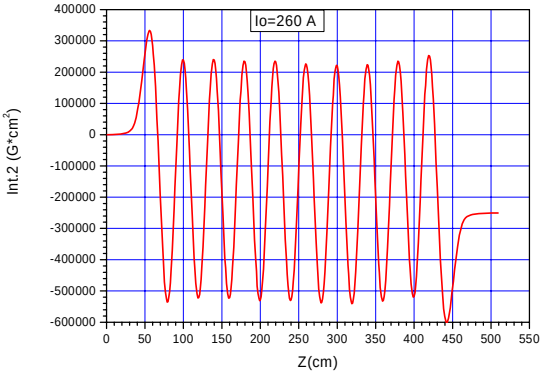
Io=260 A
Int.2 (G*cm²)
Z(cm)

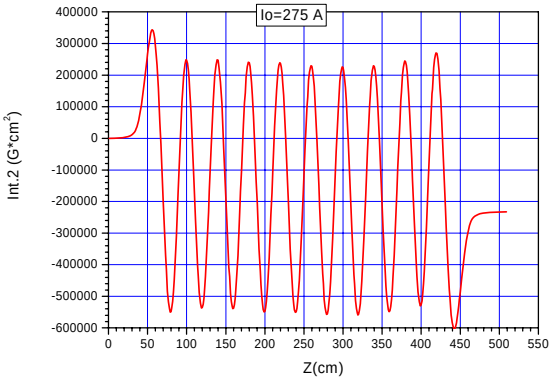
Io=275 A
Int.2 (G*cm²)
Z(cm)

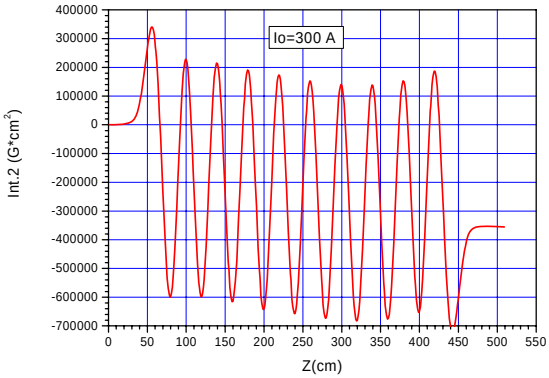
Io=300 A
Int.2 (G*cm²)
Z(cm)

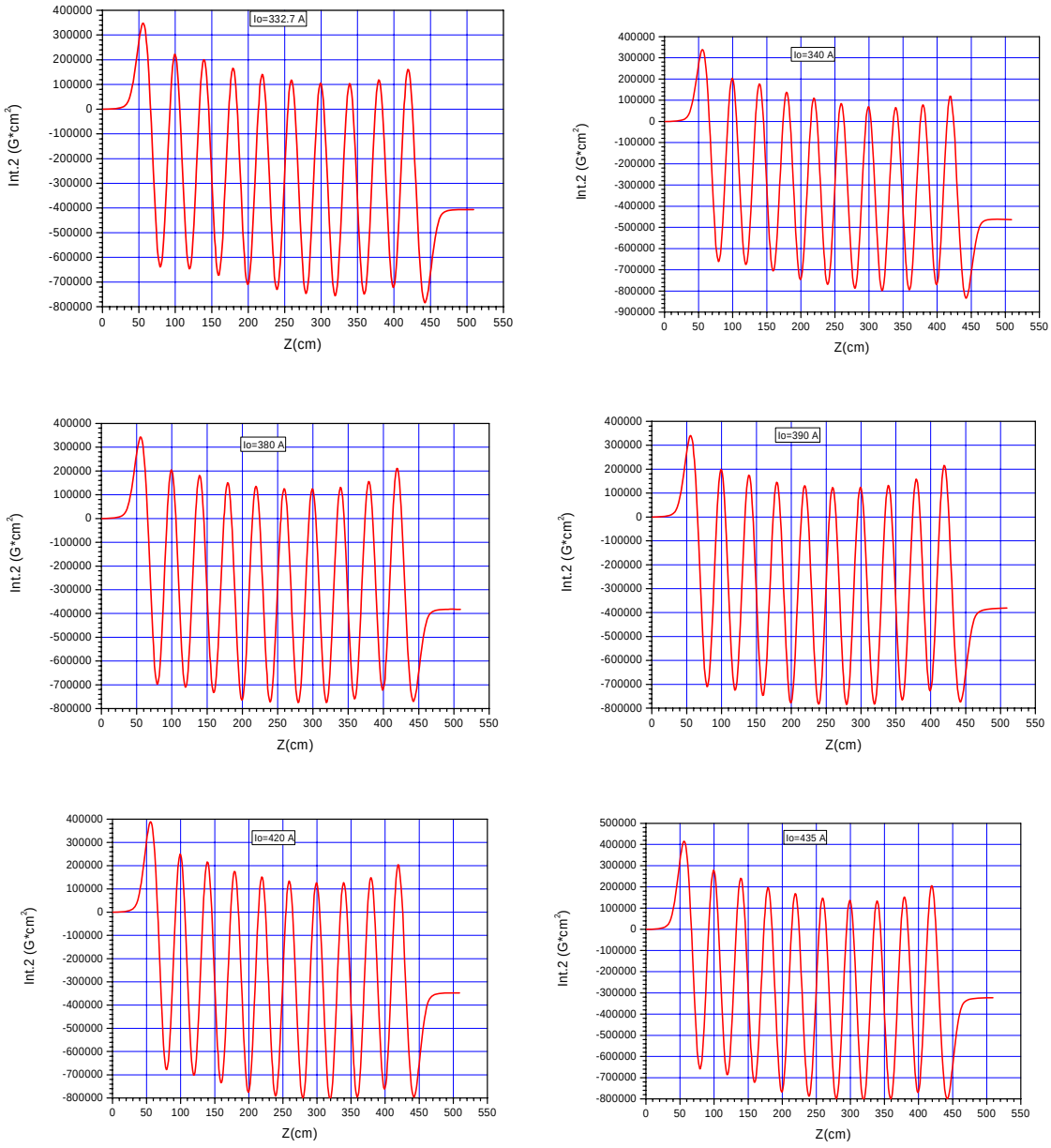

Acknowledgments

The help of Claus Jaekel, Peter Nommensen, Piotr Bartkiewicz and Vitali Kocharyan in setting up the control system for operation of the undulator in the measurement hall at DESY is acknowledged with pleasure. Markus Tischer provided valuable advice in defining the measurement program. Mikhail Yurkov kindly provided helpful comments and guidance all along the infrared undulator project.